

**BIOMIMETIC APATITE COATING ON 3D PRINTED
SCAFFOLDS FOR BONE TISSUE ENGINEERING
APPLICATION**

by

Anılcan ÇAKIR

B.S., in Metallurgical and Materials Engineering, Istanbul Technical University, 2018

Submitted to the Institute of Biomedical Engineering

in partial fulfillment of the requirements

for the degree of

Master of Science

in

Biomedical Engineering

Boğaziçi University

2020

ACKNOWLEDGMENTS

Some connections drift us to places different than our comfort zones and even give us a chance to meet new faces, live new experiences. When you look back at the end, you could not possibly understand how did you moved through those paths, nevertheless you become grateful. I am so grateful for involving this study. That's why I would like to thank my beloved teachers Kadriye TUZLAKOĞLU and Bora GARİPCAN for the massive guidance and vast experience they share during my big master adventure and cheers to their long lasting friendship because without it this wonderful cooperation could not happen in the first place.

I am very grateful for meeting Zehra Betül AHİ and Nergis Zeynep RENKLER DEĞİRMENÇİ. These wonderful people are more than laboratory coworker, they became sincere friends to me and made every struggle look so easy. These two kind women did not even hold one tiny information for themselves, just open heartily shared everything. You are the best I am so lucky to have you.

When you are stuck, every help is a bliss and should not be taken for granted. Şule ARICI and Esra GUBEN became my guardian angels whenever I got confused. Their help always became what I was just looking for and their friendship let me move forward. I wish for you the best girls. Sometimes even a small talk or sharing the day lifts the weight of the day. My upmost gratitude goes to Alp ŞARKIŞLA, Merve Begüm KÖKSAL, Aml KESKİN and Erdem Recep DEMİRCAN and to so many others just said hi and made my day better.

For my family, expressing gratitude or saying thanks is not even enough. Just their existence is a fortune on my part and will be huge support throughout my life. To my over-ambitious mother Zahide ÇAKIR, always dramatic father Kenan ÇAKIR, my technical support Necmi Mert ÇAKIR and Naci Berk ÇAKIR. Love you all guys.

ACADEMIC ETHICS AND INTEGRITY STATEMENT

I, Anılcan Çakır, hereby certify that I am aware of the Academic Ethics and Integrity Policy issued by the Council of Higher Education (YÖK) and I fully acknowledge all the consequences due to its violation by plagiarism or any other way.

Name :

Signature:

Date:

ABSTRACT

BIOMIMETIC APATITE COATING ON 3D PRINTED SCAFFOLDS FOR BONE TISSUE ENGINEERING APPLICATION

Bone-like apatite coating of polymeric materials by biomimetic coating to enhance their bone tissue healing capability is a very successful technique used in bone tissue engineering. Creating a favorable environment for cells of the bone tissue by forming an apatite layer is one of the best approaches for controlling the cell response. The purpose of this thesis is to obtain a bone-like apatite layer onto 3D printed [Polylactic Acid (PLA)/Polycaprolactone (PCL); (70/30 w/w)] blend polymer scaffolds by means of using a simple biomimetic coating process and also to determine the most effective pretreatment and coating process. Before coating pretreatment was applied to all scaffolds with 1M NaOH alkaline solution and then 0.2M $CaCl_2$ and K_2HPO_4 solutions respectively to improve Ca-P layer attachment and formation. Simulated body fluid (SBF) was utilized to mimic physiological conditions of the body throughout immersion duration of the samples which were eventually observed under scanning electron microscopy (SEM) for their morphological development on the 8th, 14th and 21th days. Ca-P development on the scaffolds was confirmed with Electron Dispersive Spectroscopy (EDX) and X-ray diffraction (XRD).

Keywords: CPCs, CMC, Calcium sulfate, Composite, Bone, Biocompatibility

ÖZET

KEMİK DOKUSU MÜHENDİSLİĞİ UYGULAMALARI İÇİN 3B DOKU İSKELELERİNİN BİOMİMETİK APATİT KAPLANMASI

Kemik dokusunu iyileştirme kabiliyetlerini artırmak için polimerik malzemelerin biyomimetik kaplama ile kemik benzeri apatit ile kaplanması, doku mühendisliğinde kullanılan oldukça başarılı bir tekniktir. Apatit tabakası oluşturarak kemik dokusu hücreleri için uygun ortam yaratmak, bu hücre davranışını kontrol etmek için en iyi yaklaşımlardan biridir. Bu çalışmanın amacı, biyomimetik kaplama yöntemi yardımı ile kemik benzeri apatit bir yapıyı [Polilaktik Asit (PLA)/Polikaprolakton (PCL); (70/30 w/w)] karışım bir polimerden elde edilmiş ve 3 boyutta basılmış bir doku iskelesi üzerinde elde etmektir. Ayrıca bu kaplama tekniği için en etkili ön işlem ve kaplama parametrelerini bulmaktır. Kaplama öncesi tüm doku iskelelerine 1M NaOH alkalın çözeltisi ve ardından Ca-P tabakasının yapışmasını ve oluşumunu iyileştirmek adına sırasıyla 0.2M $CaCl_2$ ve K_2HPO_4 çözeltileri ile ön işlem uygulandı. Doku iskelelerinin Ca-P kaplanması sırasında simüle edilmiş vücut sıvısı yardımı ile vücudun fizyolojik ortamına benzer bir ortam elde edilmeye çalışıldı. 8, 14 ve 21. gün sonlarında iskele yüzey morfolojileri SEM yardımı ile incelendi. Ayrıca iskele üzeri Ca-P tabakasının varlığı Enerji Dispersiv Spektrum (EDX) ve X-Işını Difraktometresi (XRD) analiz yöntemleri yardımıyla kanıtlandı.

Anahtar Sözcükler: CPCs, CMC, Kalsiyum sülfat, Kompozit, Kemik, Biyouyumluluk

TABLE OF CONTENTS

ACKNOWLEDGMENTS	iii
ACADEMIC ETHICS AND INTEGRITY STATEMENT	iv
ABSTRACT	v
ÖZET	vi
LIST OF FIGURES	ix
LIST OF TABLES	xii
LIST OF SYMBOLS	xiii
LIST OF ABBREVIATIONS	xiv
1. INTRODUCTION	1
1.1 Motivation	1
1.2 Objective	4
1.3 Outline	4
2. BACKGROUND	6
2.1 Bone Structure	6
2.2 Bone Biology	7
2.3 Bone Deformation and Healing	8
2.4 Tissue Engineering	9
2.4.1 General Methods for Tissue Engineering	10
2.4.2 Tissue Engineering for Bone Tissue	10
2.4.3 Simulated Body Fluid (SBF)	11
2.4.4 Scaffolding with 3D Printers	13
2.4.5 Bone Grafts and Bone Substitutes	13
2.4.5.1 Autograft	14
2.4.5.2 Allograft	14
2.4.5.3 Xenograft	15
2.4.5.4 Metals and Their Alloys	15
2.4.5.5 Ceramics	15
2.4.5.6 Polymers	16
3. MATERIALS AND METHODS	19

3.1	3 Dimensional Tissue Scaffold Production	19
3.2	Material Selection and Application of 3D Printing	20
3.3	Surface Modification	22
3.3.1	Alkaline Solution Treatment	22
3.3.2	$CaCl_2$ and K_2HPO_4 Solution Treatment	23
3.4	Preparation of Simulated Body Fluid	23
3.5	Optimization and Application of Biomimetic Coating	24
3.6	Material Characterization	25
3.6.1	Scanning Electron Microscopy (SEM)	25
3.6.2	Energy-Dispersive X-ray Spectroscopy (EDX)	26
3.6.3	X-ray Diffraction Spectroscopy (XRD)	26
3.7	Cell Culture Studies	26
3.7.1	Sterilization of Scaffolds	27
3.7.2	Cell Seeding Process	27
4.	RESULTS AND DISCUSSION	28
4.1	Material Selection	28
4.2	Surface Modification	30
4.2.1	Effects of Alkaline Solution	30
4.2.2	Effects of $CaCl_2$ and K_2HPO_4 Solutions	32
4.3	Effects of Simulated Body Fluid on Coating Quality under Continuous Agitation and Periodic Solution Renewing	33
4.4	EDX Analysis	36
4.5	XRD Analysis	39
4.6	<i>InVitro</i> Cell Culture Studies	44
5.	CONCLUSION	46
	REFERENCES	47

LIST OF FIGURES

Figure 2.1	Bone Interior Structure	6
Figure 2.2	Bone Regeneration Process [27].	8
Figure 2.3	Designing steps of successful tissue scaffold.	9
Figure 2.4	Mechanism behind SBF solution and Scaffold surface [38].	12
Figure 2.5	Graft types [4].	14
Figure 2.6	Molecular Structure of PLA [43].	18
Figure 2.7	Molecular Structure of PCL [36].	18
Figure 3.1	Scaffold design created with the help of SolidWorks software then integrated for 3D printers by CURA software.	19
Figure 3.2	I: Layer one, II: Combination of two perpendicular layers, III: 45° third layer and IV: Final printed version of the designed scaffold.	20
Figure 3.3	Single Extrusion 3D printing machine (Ultimaker 2-Go, Ultimaker, Netherlands).	21
Figure 3.4	Experimental set-up for agitated group.	24
Figure 3.5	Experimental set-up for biomimetic coating.	25
Figure 4.1	Printed final scaffolds.	28
Figure 4.2	After 14 days of immersion, i) PLA scaffold surface, ii) PLA/PCL blend scaffold surface. (Left: 200X, Right side: 2000X magnification).	29
Figure 4.3	SEM images of PCL/PLA blend scaffolds after application of alkaline and $CaCl_2$ and K_2HPO_4 solutions with varying duration; A)1M alkaline treatment for 1h. B)3M alkaline treatment for 3h. C)1M alkaline treatment for 3h. D)3M alkaline treatment for 1h (250X).	31
Figure 4.4	SEM images of PCL/PLA scaffold sample surface without solution treatment (A) and same sample with surface treatment by consecutive solution dipping (B) (Upper images: 1000x, lower images: 10.000x magnification).	32

Figure 4.5	8 th day SEM images. S8: Still group, R8: Solution Renewed group, A8: Agitated group (Upper images: 2000x, bottom images: 20.000x magnification).	33
Figure 4.6	14 th day SEM images. S14: Still group, R14: Solution Renewed group, A14: Agitated group (Upper images: 2000x, bottom images: 20.000x magnification).	34
Figure 4.7	21 th day SEM images. S21: Still group, R21: Solution Renewed group, A21: Agitated group (Upper images: 2000x, bottom images: 20.000x magnification).	34
Figure 4.8	SEM image of PCL/PLA Scaffold that constantly agitated during 21 days SBF immersion (50.000x magnification).	35
Figure 4.9	SEM image of interior layer of PCL/PLA scaffold after 14 days of SBF immersion (200x magnification).	36
Figure 4.10	EDX graphs for still samples for 8 th (S8), 14 th (S14) and 21 th (S21) days.	37
Figure 4.11	EDX graphs for solution renewed samples for 8 th (R8), 14 th (R14) and 21 th (R21) days.	38
Figure 4.12	EDX graphs for solution agitated samples for 8 th (A8), 14 th (A14) and 21 th (A21) days.	38
Figure 4.13	XRD spectra of all HA coated sample groups according to their SBF immersion conditions and duration times.	39
Figure 4.14	XRD spectra of three sample groups after 8 days of SBF immersion.	40
Figure 4.15	XRD spectra of three sample groups after 14 days of SBF immersion.	41
Figure 4.16	XRD spectra of three sample groups after 21 days of SBF immersion.	41
Figure 4.17	XRD spectra of Still sample groups according their duration in SBF solution.	42
Figure 4.18	XRD spectra of Renewed sample groups according their duration in SBF solution.	42
Figure 4.19	XRD spectra of Agitated sample groups according their duration in SBF solution.	43

Figure 4.20	14 day SEM images (Upper images; without coating, lower images; with Ca-P coating on the surface).	44
Figure 4.21	14 day SEM images of cells attached to Ca-P coated surface.	45

LIST OF TABLES

Table 2.1	Comparison Between Simulated Solution and Body Ion Concentration [1].	12
Table 2.2	Physicochemical, mechanical and biological properties of HA [15].	16
Table 3.1	Optimized 3D printer parameters.	20
Table 3.2	Simulated Body Fluid Material Content (Sigma Aldrich, Germany) [1].	24
Table 4.1	Surface Treatment Groups.	30

LIST OF SYMBOLS

HCO^{3-}	Bicarbonate
Ca^{2+}	Calcium Ion
$CaCl_2$	Calcium Chloride
Cl^-	Chloride Ion
H^+	Hydrogen Ion
OH^-	Hydroxide Ion
HPO_4^{3-}	Hydrogen Phosphate
Mg^{2+}	Magnesium Ion
K^+	Potassium Ion
K_2HPO_4	di-Potassium Hydrogen Phosphate
KCl	Potassium Chloride
SO_4^{2-}	Sulfate
$NaCl$	Sodium Chloride
$NaOH$	Sodium Hydroxide
$NaHCO_3$	Sodium of Hydrogen Phosphate
Na_2SO_4	Sodium Sulfate

LIST OF ABBREVIATIONS

2D	Two Dimensional
3D	Three Dimensional
AGT	Agitated Sample Group
CAD	Computer Aided Design
CNT	Control Group
DMEM	Dulbecco's Modified Eagle Medium
ECM	Extracellular Matrix
EDX	Electron Diffraction Spectroscopy
FTIR	Fourier Transform Infrared Spectroscopy
HA	Hydroxyapatite
PBS	Phosphate Buffered Saline
PCL	Polycaprolactone
PLA	Polylactic Acid
RNW	Renewed Sample Group
SEM	Scanning Electron Microscope
SBF	Simulated Body Fluid
STL	Still Sample Group
UV	Ultraviolet
XRD	X-ray Diffraction Spectroscopy

1. INTRODUCTION

1.1 Motivation

Tissue engineering has a goal to restore and assist self-healing of tissue that lost its function due to illness or trauma. It is a very promising approach in especially bone tissue medication to achieve healing and assisting for bones that unable to regenerate themselves [1]. In this quest, tissue engineering is always looking for the better substitutes for materials that have drawbacks or improve performance by enhancing their properties [2, 3].

Even though bone has an excellent self-repairing property, still there are many serious physical or pathological deformities that may not be fully healed without external aid [1]. The use of bone graft is the golden standard for treating skeletal diseases and defects. The most common graft type is autograft. However, bone autografts bear serious disadvantages regarding requirement for second surgical operation and risk of donor site morbidity [4]. Even the source of autograft is patient's own body, still there is high possibility of serious complications such as pain, infection, scarring, blood loss [5]. On top of that, acquiring and working on autograft to create a medium for bone growth are not always possible in the case of infectious diseases because for all patients, size, shape and conditions of damaged tissue will be considerably different. Treating without including these factors can lead to improper healing and even additional surgeries [5, 1]. Apart from old methods, with the new advancements in technology, 3 dimensional (3D) printers are allowing us to work around these factors by manipulating bone scaffolds to patient specific needs.

Porous solid biomaterials in 3D form are called as scaffold which has direct relation with the cell adhesion, gas and nutrient diffusion and cell-material interaction in the tissue area [6]. Scaffolds are acting as a starting area for regeneration and creating mechanical support for the newly formed tissue [7]. Due to its flexible product param-

eters in terms of size, shape, thickness, texture design, material type and so on, day by day popularity of bio-printers are increasing [8, 9]. Production of highly effective scaffold starts with feeding the right material to printer. Any synthetic material suitable to replace the damaged bone should have a combination of biological and mechanical properties: bioactivity, biodegradability and sufficient mechanical strength [5].

Degrading overtime is the key factor for bone tissue engineering so even though metals and ceramics have excellent bioactivity, their non-degradability is creating a problem and leading the industry to polymeric materials for scaffold designing. For example, Poly-lactic acid (PLA) shows mechanical properties very similar to human bone and on top of that it is biodegradable by hydrolysis that new formed tissue can easily invade the space that degrades from PLA scaffold [3, 4]. On the other hand, PLA is highly hydrophobic and lacks nucleation sites so the fact is in terms of surface properties, PLA are not completely compatible with biological applications [10]. Polycaprolactone (PCL) has a slow degradation than PLA that's why it is also very good candidate for bone tissue engineering where scaffolds should maintain their integrity up to 6 months [7, 11]. PCL is highly bio-compatible and easily shapeable due to its low melting point but its applications are limited by its low tensile strength and young modulus [12]. PLA has superior mechanical properties than PCL. Both polymers have serious advantages and disadvantages in bone tissue engineering area. That's why as previously studied, blending option of these polymers will have benefits for the design of hydroxyapatite coated bone tissue scaffolds [13].

The tissue and its unique environment should be fully understood and skillfully replicated to reach best possible healing effectiveness. Suitable surface chemistry is the first step for successful cell attachment and proliferation for bone tissue recovery [14]. In this thesis we were working with MC3T3 bone cell line and in order to reach complete proliferation and cell differentiation they are favoring specific types of surface properties. Due to its promotion to osteoconductivity and excellent bio-activity, it is well known that calcium phosphate (Ca-P) structure such as calcium hydroxyapatite, is highly utilized to mimic the inorganic components of bone [15]. Ca-P based materials can promote bone cell attachment and growth without creating toxic effect or harming

surrounding tissue. Hydroxyapatite (HA) is consisted of the 70% of the inorganic phase of whole bone [16, 4, 15] that this familiarity between bone tissue and hydroxyapatite can be counted as the biggest advantage of the HA structure.

There are several coating techniques that can form stable hydroxyapatite structure on the polymeric scaffold surface such as thermal spraying, sputter coating, sol-gel deposition, hot isostatic pressing and dip coating [7, 4]. On the other hand, designed scaffolds have to withstand the coating technique's process requirements such as high temperature, mechanical stress and physical deformation thus it needs to be stable and undamaged after coating procedure. It was concluded that biomimetic coating technique is the most suitable process in order to coat 3D printed polymeric scaffolds that designed to be implanted to improve tissue healing of the body. Simulated Body Fluid (SBF) is a supersaturated solution that designed to mimic original body fluid. Only by using SBF solution 3D printed complex structures can be coated uniformly. This coating technique also supports biologic conditions similar to body like pressure, temperature and pH [4, 3].

Biomimetic coating includes several pre-surface modifications to improve final coating quality. Previous studies shows that treating with NaOH solution leads exposure of more hydroxyl functional groups thus increase in Ca^{+2} binding property on scaffold surface [17]. Calcium ions act as nucleation sites, initiation points for apatite coating procedure [10]. After modification of scaffold surfaces, SBF was used to form hydroxyapatite structure throughout PLA/PCL blend scaffold samples. At the same time, due to SBF immersion technique is a very time-consuming process as reported in many previous studies, so there were few process optimization included in order to reduce coating time. Few approaches like agitation and solution renewing were advised for altering immersion time [14]. Scaffolds were immersed in separate falcon tubes that categorized for their immersion days (8, 14, 21) and immersion types (still, agitated, solution renewed).

And finally, thesis project included cell culture study in order to test these advanced scaffolds in terms of their bone cell viability. Pore size, porosity, surface area

and interconnectivity are the few important parameters that is directly effecting cell seeding capability of scaffolds [7]. So several test were included in order to measure mentioned properties. During incubation, there were several control points at 7th and 14th. In these points cells were dyed with MTS assay that is a calorimetric method for sensitive quantification of viable cells. By dying cells their absorbance rate were controlled under 490 nm which gives general information about cell growth on samples.

1.2 Objective

The aim of the this thesis is to create alternative solution to bone graft by producing bio-compatible polymeric scaffolds coated with calcium phosphate (Ca-P) structure which are 3D printed by blend filament [PLA/PCL; (70/30 w/w)] then coated by biomimetic approach.

General steps can be summarized as;

- Designing and printing polymeric scaffolds with approximate 800 μm porosity.
- Achieving biomimetic coating of scaffolds in freshly prepared Simulated Body Fluid solution.
- Determining the best biomimetic coating type and immersion duration among several sample groups.
- Supporting the attachment of the MC3T3 cells on scaffolds.

1.3 Outline

This thesis has 5 chapters. Starting chapter, includes the motivation of the study and objectives. Following chapter 2, includes required background information about structure and biology of the bone, standard bone tissue engineering solutions.

Chapter 3 states the used materials and utilized methods. Experiment results and discussions are shared in chapter 4. Finally, in chapter 5 conclusion is presented.

2. BACKGROUND

2.1 Bone Structure

Bone is a very important tissue that has variety of duties in body such as mechanical support, organ protection, muscle binding and mineral storage. Bone has a dynamic structure and it constantly undergoes growing, regeneration and renewing. In order to take care of these necessities bone cells are constantly demolished and rebuilt [18]. Bone has a structure consisting water (8%), organic matrix (22%) and mostly mineral matrix (70%). In organic matrix of bone formed by hydroxyapatite (HA) crystal structure, citrate, sodium, magnesium, fluoride and calcium phosphates. Balance between these ratios has determining factor on bone's mechanical stability. Bone can be divided into two parts as cortical (compact) bone (80%) and trabecular (elastic) bone (20%) (Fig. 2.1) Compact part is tough and dense so it surrounds and protects whole bone structure, on the other hand elastic bone has porous structure and more surface area so it mainly gives impact dampening capability and internal stability to bone. They both work together and reduce mechanical stress and work load on complete bone structure [19, 20].

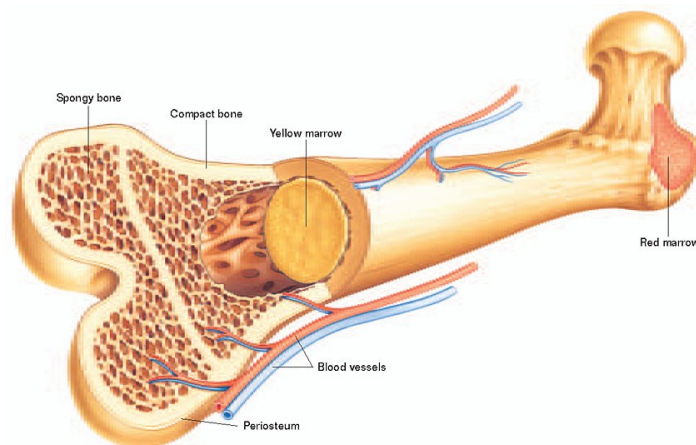


Figure 2.1 Bone Interior Structure from [4].

Microscopically, bone has an excellent internal dynamic with web-like design that includes functional cells and extracellular matrix (ECM). ECM can be divided

into organic (collagen, elastin, polysaccharides) and inorganic parts (calcium phosphate nanocrystals). Main purpose of ECM provides three-dimensional structure for cells to support their movement and proliferation [21]. Organic matrix of bone includes type-I collagens and other non-collagen proteins such as glycoproteins, proteoglycans, peptides, carbohydrates and lipids. Inorganic matrix of bone has two major functions; ion storage and providing mechanical toughness. Two thirds of bone tissue are calcium phosphate (Ca-P) and reaction of Ca-P with calcium hydroxide leads hydroxyapatite crystal. The remaining portion is mainly collagen structure. Bone cells just takes 2% of the total bone weight. This brittle apatite mineral is not only but most critical formation in bone. Reduction in HA crystallinity directly effects the bone reformation capabilities that leads homeostasis. Mimicking and creating replication of bone like structures are depending on the knowledge about HA structure and its natural formation in bone structure [22, 23].

2.2 Bone Biology

Healthy bone cells are constantly in perfect harmony which is called as bone homeostasis. To maintain that state there are different types of cells in play that all are related with mesenchymal cells. These cells are osteoblasts, osteoclasts, and osteocytes. Osteoblasts are in charge of bone formation. These cells (osteoid) secrete matrix proteins and type-I collagen which are not yet mineralized [24]. Calcification of bone is another duty of osteoblasts. Secreted proteins can hold minerals such as calcium and phosphate in order to form final hydroxyapatite phase. Osteoclasts partake in bone remodeling by using specific enzymes which can dissolve mineral phase and collagens thus regulating bone mass. Another cell is osteocyte which is derived from osteoblasts. It is mainly responsible for internal communication and coordination. Hormonal and mechanical stimulation can be detected by osteocytes and this phenomena leads remodeling procedure with the coordination between both osteoblasts and osteoclasts. Coordination of these cells lead necessary changes in bone mass to compensate mechanical loads [22, 18].

2.3 Bone Deformation and Healing

Mechanical instability, bone density loss or osteoporosis could be listed as few of many reasons for bone fracture. Fractures can be investigated under three groups as comminuted, simple and stress fractures. In comminuted fractures, bone breaks into multiple pieces due to sudden and rapid sudden forces like in traffic accidents but in stress fractures, there will be many micro level cracks and damages formed over time due to repeating low magnitude force effecting the bone [25].

Healing of the bone can be defined as returning to previous mechanical and physical state of bone before injury or trauma. Complete healing is a long process that has several important steps (Fig. 2.2). These steps are inflammation, recovery and reformation which all starts with cellular responses. Fracture region increases its cellular activity during first 24 hour then slows down during healing period which takes weeks or even years depending on the fracture type. Around fracture, first cartilage like structure called as callus forms. Callus is not capable of withstanding compression and torsion movements before hardening by mineralization [26].

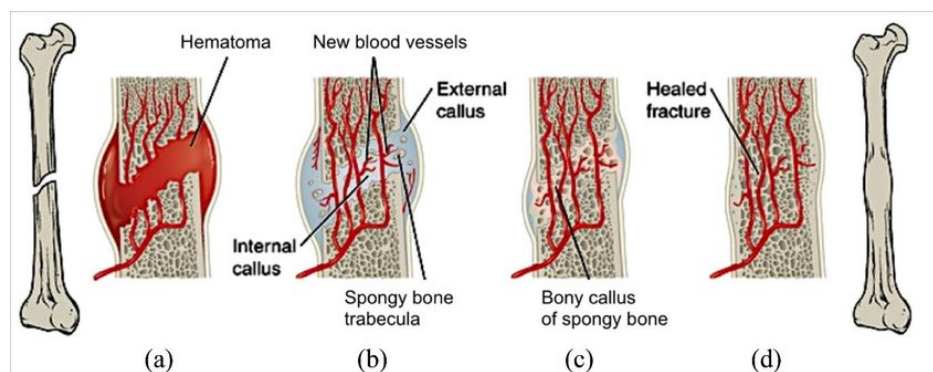


Figure 2.2 Bone Regeneration Process [27].

Mineralization phase is important to give mechanical stability to bone during complete healing process. Reformation of bone happens in response to stress comes from body, so that way bone regulates its density and diameter [25].

2.4 Tissue Engineering

Due to trauma, diseases or congenital problems there is constant need for substitutes to repair or replace biological systems as tissues and organs. In the case of damages above the threshold of bone's self-repair capability, need for external aid arises. Many developments have been achieved in the pursue of finding optimum advanced material and achieving fabrication of devices to be used in the field of tissue engineering. Even though autologous bone grafts are considered the most suitable approach to bone defects, there are few serious problems waiting to be solved which are donor site morbidity, low mechanical performance of implanted graft, long recovery period and need for complex graft shapes [28].

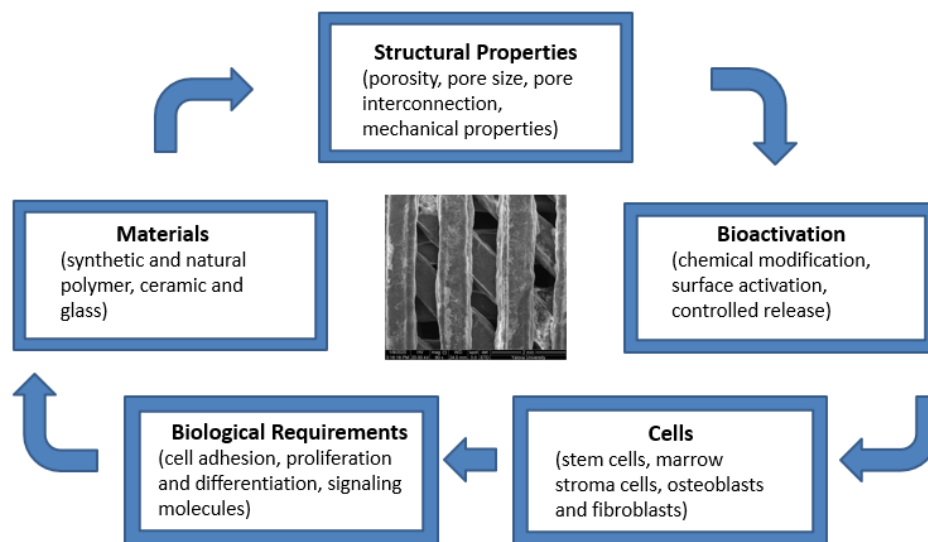


Figure 2.3 Designing steps of successful tissue scaffold.

Apart from classical biologic approach, tissue engineering depends on self-regeneration and formation. Instead of applying limited implants, the goal is creating functional tissues for specific needs. Cells are following the previously formed structure if suitable guide and environment is provided. Guiding the tissues for our necessities by understanding their behavior during natural healing process is the main key factor for tissue engineering. So the concept of tissue engineering depends on the creation of scaffold structure, which has appropriate physical, chemical and mechanical properties in order to enable cell migration and tissue formation in three dimensional environment.

Providing these environmental cues help cell proliferation in the specific ways [29, 30].

2.4.1 General Methods for Tissue Engineering

Overall, tissue engineering concept starts with the isolation of specific cells from healthy tissue and then continues with their seeding process on suitable 3D environment to let them cultivate on scaffolds. After implantation, the scaffold will degrade over time in predetermined rate to let newly formed tissue to take its place [11]. Success of any tissue or organ study depends on these factors;

- Having an ability of stem cells that can differentiate into specific cell types.
- Providing required biological and mechanical support for cell attachment and proliferation.
- Introducing growth factor that will benefit cellular activities.

More the similarity between scaffold and original tissue better the cellular attachment and migration thus overall tissue generation success. Cells are very sensitive to their environmental cues which are the core idea for tissue engineering applications [31]. Designing successful tissue scaffold depends on several important steps that they all have huge importance on mimicking and developing engineered tissue (Fig. 2.3). Controlling these cues such as surface topography, chemical response, ECM likeness of scaffold, mechanical stress and leading proteins, will be determining step for cell differentiation and formation of desired functional tissue structure [11, 7].

2.4.2 Tissue Engineering for Bone Tissue

Grafting approach is still a valid method and accepted as golden standard for bone tissue related diseases. However, the lack of donor, pathogen risk and immuno-

genic rejections are still major problems that are waiting to be solved [32, 5]. That's why tissue engineering, especially in bone tissue area, is rapidly advancing.

Bone tissue is one of the most complex tissue in body that its specialized structure invites complications even in conventional surgical application. Bone tissue engineering is the better way to form stable, complex and functional tissues that can be produced by the combination of suitable scaffold environment and osteoblast cells [30]. Attachment, differentiation and mineralization of cells serve as foundation of new bone tissues. Few of the important aspects of mentioned scaffolds are its biocompatibility, biodegradability and porous structure [33, 34]. Biocompatibility effects interactions between material surface and cell. Degradation is also critical feature because 3D construct should give out its place to newly formed healthy tissue by degrading overtime in proper rate. And lastly porous structure of scaffold has direct relation with osteoconduction of cells which are attach to surface and migrates throughout healing process [1].

Many materials and their combinations are investigated to reach most optimized material in the field [6]. Metals and ceramics are both used for many applications but their lack of degradation in biological environment and being hard to handle for delicate applications, made these materials less popular among other options. On the other hand, polymer or polymer-based materials can be easily tailored to specific needs in terms of surface quality, shape, weight, functional behaviors, controllable degradation rates and so on [35]. These serious advantages made polymers huge interest in bone tissue engineering field [36].

2.4.3 Simulated Body Fluid (SBF)

SBF solution was proposed initially by Kokubo [37], present an ionic composition similar to human blood plasma, and has been widely used to test the bioactivity of different materials in-vitro. SBF solution is a supersaturated solution that has a nearly identical ion concentration as human blood plasma. The detailed comparison between

natural body ion concentration and solution ion concentration can be seen in Table 2.1. SBF solution supports surface coating and create a suitable surface for bone cells. Cells will attach the more familiar surface in this case HA surface is very similar to natural bone structure. Ion exchange process and following bone cell migration and attachment can be seen in Figure 2.4.

Table 2.1
Comparison Between Simulated Solution and Body Ion Concentration [1].

Ion types	Body Ion Concentration (mM)	Solution Ion Concentration (mM)
Na ⁺	142.0	142.0
K ⁺	5.0	5.0
Mg ⁺	1.5	1.5
Ca ²⁺	2.5	2.5
Cl ⁻	103.0	147.8
HCO ³⁻	27.0	4.8
HPO ₄ ³⁻	1.0	1.0
SO ₄ ²⁻	0.5	0.5

This unique solution consists of many different chemicals and inappropriate preparation conditions can lead early precipitation of apatite or any other compound and ruin whole solution concentration balance. In this case it will deviate from intended human plasma likeness. Final solution should be colorless and transparent and has 30 days before expiration .

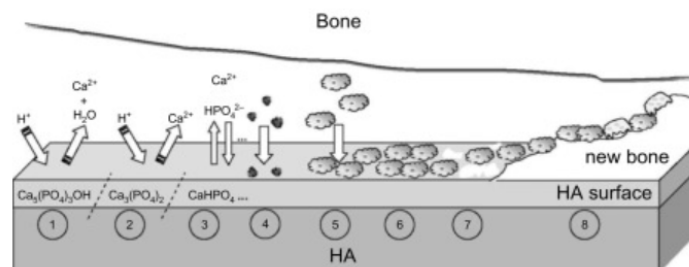


Figure 2.4 Mechanism behind SBF solution and Scaffold surface [38].

2.4.4 Scaffolding with 3D Printers

Using 3D printers can be categorized under rapid prototyping technique that whole process supervised under computer support that's why this technique is much more controllable and advanced than other prototyping methods. With rapid prototyping 3D scaffolds can be built with ease. With the bottom-up filling process, solid 3D structure can be formed layer by layer thus creating designed scaffold (Fig. 3.1). Creating intended structure depends on several important parameters such as temperature, material flow, printing speed and so on. Size, shape, geometry, pore size and even their interconnectivity could be altered by fine tuning of these variables. With this freedom in hand, popularity of rapid prototyping is increasing day by day. Furthermore, ease of material selection and application, increases the possibility of controlling possible biological responses and degradation kinetic [8, 39].

2.4.5 Bone Grafts and Bone Substitutes

Bone grafts are implantable material or combination of materials that helps bone regeneration by their osteogenic and osteoinductive properties [40, 6, 5]. Tissue engineering approach utilizes synthetic or natural materials in order to meet biologic and mechanical needs of the application area. Osteogenic materials are capable of proliferation and differentiation of bone cells by triggering required signals and cell stimulation. Cells are differentiate into mature osteoblasts, if osteoinductive properties guide them. In literature there are many different applications utilizing variety of materials. They are chosen according to application needs and material properties. Bone scaffolds are designed to lead cells into migration, adhesion, differentiation and proliferation in 3 directional environments. Especially bone scaffolds have to bear required pores and canals that will improve ECM likeness with natural bone tissue. And also scaffold should be dissolvable in body without harm that will eliminate second surgical operation and its risks. New tissue will cover the scaffold through canals and pores that will lead vascularization on region. Previous studies suggest porosities around 800 μm is optimum range for this kind of applications [41, 42].

One of the important aspects for bone graft materials is surface characteristics of implant. Its topography, surface energy, chemical formation, wettability and surface activity are deciding factors for many biological responses in body [43].

2.4.5.1 Autograft. In bone tissue engineering applications this method generally accepted as a gold standard. Autografts is taken from patient's own body and re-implanted into a damaged tissue. The most advantageous side of this application is near zero immune response. This is quite understandable because, the origin of grafts is patient's own body. This will reduce rejection risk of implant to minimum. On the other hand, infection risk at the region that graft is taken and during operation death of surrounding tissue are the two major disadvantages of this approach. In these cases donor site could suffer more than damaged area and could render whole operation pointless. Lastly suitable and applicable donor is limited inside body thus search for new solutions are required [26].

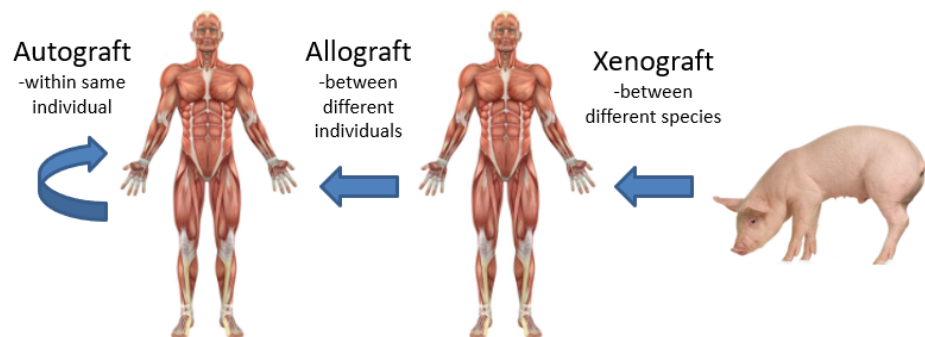


Figure 2.5 Graft types [4].

2.4.5.2 Allograft. One of the other grafting solutions in tissue engineering is allografts. These grafts are acquired from another donor body or cadaver then processed under freezing or lyophilizing to avoid contamination from donor site. Apart from autografts which require second surgery, allografts need one surgery. This reduces infection and donor site morbidity risk. But taken tissue from another immune system could react in new body and lead implant failure [44, 32].

2.4.5.3 Xenograft. Xenografts are grafts that are removed from one species and implanted into another species. Inorganic bovine bone is generally used as a xenograft in bone therapy. These grafts are subjected to chemical and thermal processes in order to be purified from the organic structures they contain. They consist almost entirely of hydroxyapatite and have similar properties to human bone. Their mechanical strength is very low. Since the xenografts can be easily broken, they can provide limited mechanical support during the bone healing process and are difficult to use in surgical operations. They are not useful because the risk of immunity is high. Osteoinductive properties are lost due to the removal of active proteins during deproteinization processes to reduce the risk of immune [27].

2.4.5.4 Metals and Their Alloys. For many years metals and their alloys have been used as implant material due to several important reasons. First their mechanical strength and mouldability make them very suitable for bone applications. Titanium and stainless steel are the general choice for bone fracture fixation applications. However, elastic modulus of used metals could lead a problem known as stress shielding which is huge difference in elastic modulus between bone and implanted metal. Even though corrosion resistance is very high, there is always a risk for corrosion and leading into inflammatory response then finally implant failure. Although they can be fixated on specified region, they do not have any osteoconduction ability that implant may become loose with time [23].

2.4.5.5 Ceramics. Ceramics are very customizable materials that their applications varies according to their bioactivity. They can be categorized as bioinert (zirconia, alumina), bioactive (HA, bioglass) and bioresorbable [23]. Most known and used ceramics are alumina and zirconium in field. Even though they are highly brittle and bearing low endurance, they have excellent hardness, corrosion resistance and biocompatibility. Chemical and biological similarity of some ceramics such as hydroxyapatite and tricalcium phosphate, made them excellent candidate for bone tissue applications [23, 35].

Table 2.2
Physicochemical, mechanical and biological properties of HA [15].

Properties	Experimental Data
Chemical Composition	$Ca_{10}(PO_4)_6(OH)_2$
Ca/P molar	1.67
Crystal System	Hexagonal
Young Modulus (GPa)	80-110
Elastic Modulus (GPa)	114
Compressive Strength (MPa)	400-900
Density (g/cm ³)	3.16
Hardness (HV)	600
Decomposition Temperature (°C)	above 1000
Melting Point (°C)	1614
Biocompatibility	High
Bioactivity	High
Biodegeneration	Low
Cellular-compatiblity	High
Osteoconduction	High

Creating scaffold very close to bone is one of the important goals of tissue engineering. Although there are different ratios of hydroxyapatite ceramic, Ca/P ratio as 1.67 has the chemical and physical structure similar to bone. Previous studies showed that HA has very good osteoinduction and biocompatible properties. Problem with HA made scaffolds is its low solubility and stability (Table 2.2). Also its brittleness and processing difficulties lead usage of calcium phosphate cements (CPCs) or just coating the surface. Coating method has huge promises because it both provide mechanical support bone needs by scaffold material and bone cell adhesion and differentiation with the help of HA coated surface. Bioactive glasses are also used for the injuries about hard tissues. Their attachment to bone tissue provided by hydroxycarbonate apatite and bioactive glasses are generally used for the dental and jaw applications [35].

2.4.5.6 Polymers. Most important aspects of polymers are their highly tunable and changeable properties. This modification advantage makes polymers very favor-

able material among others. Processing is easier for complicated parts due to their high moldability and flexibility. Even their degradation rate can be controlled by diverse functional groups. They can also be activated from outer signals such as pH, temperature or enzymes. According to process needs both natural (collagen, chitosan, Glycosaminoglycan, silk fibroin, alginate) and synthetic (Polylactic acid, Polycaprolactone, polyglycolide) polymers can be selected for scaffold material. Natural polymers have high biocompatibility and low toxicity so chance for causing immunogenic reaction is quite low. However due to their mechanical properties they are hard to process. So in general they are used together with synthetic materials.

Chemically processed polymers show excellent stability and variety thus in case of specific requirements, working with synthetic polymers are better than natural polymers. Synthetic polymers are highly suitable for preparing tissue scaffold. On top of that degradation time of synthetic polymers can be tuned by blending with other polymers with different properties. Combination of both can give best results for many advanced applications. However, generally the biocompatibility of these polymers is lower than natural ones. In tissue engineering most commonly used polymers are polyglycolide (PGA), polylactic acid (PLA) and polycaprolactone (PCL) including their blends [34, 13].

- PLA chiral structure is the reason that PLA has three distinct type of polymer. These are D-PLA, L-PLA and combination of two D,L-PLA. PLA is the product of ring opening reactions of L-PLA. Melting temperature of this polymer is 185°C and glass transition temperature is 90°C . It is more hydrophobic than PGA and their general usage is in bone regeneration field with combination of HA like ceramics [45, 29].
- PCL is biodegradable and bio-compatible polymer that because of these fine features they can find many uses in treatment field. It can be found in room temperature as rubber form. Its melting point, glass transition temperature and

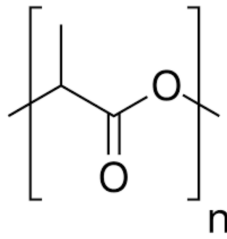


Figure 2.6 Molecular Structure of PLA [43].

decomposition temperature is respectively 60°C, -60°C and 350°C. Degradation rate of PCL is slower than PLA and PGA that's why it is more suitable for long term implant treatments. Blending with other polymers is a reasonable option [45].

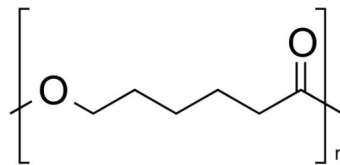


Figure 2.7 Molecular Structure of PCL [36].

3. MATERIALS AND METHODS

3.1 3 Dimensional Tissue Scaffold Production

The scaffold design is formed in order to achieve the most optimized geometry for Ca-P coating. Drafts were drawn with the SolidWorks program and made suitable for 3D printers with the printer design software CURA. First important premise for design were having suitable pore size around $800\ \mu\text{m}$ for bone tissue regeneration applications [43, 46].

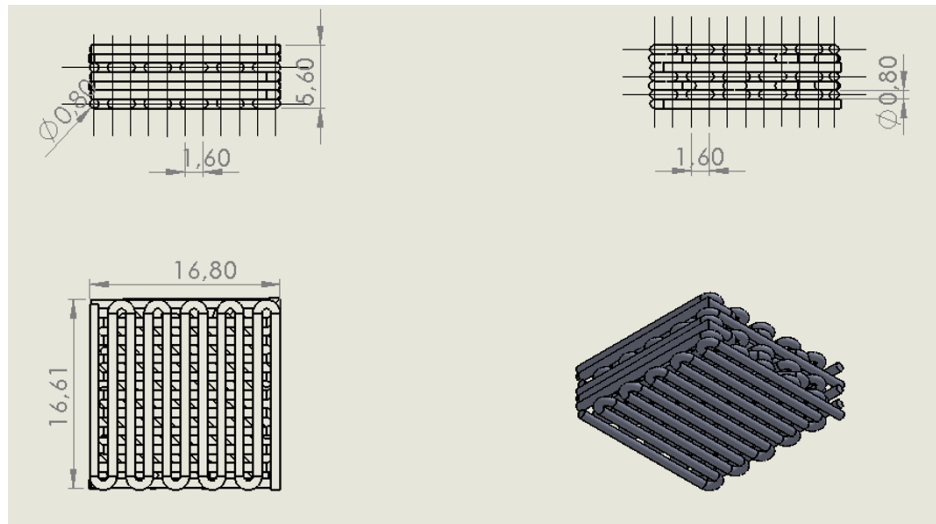


Figure 3.1 Scaffold design created with the help of SolidWorks software then integrated for 3D printers by CURA software.

In order to support that, as seen in Figure 3.2, scaffold design have 3 distinct layers that first layer stays in 90° angular to y axis then second layer stays bellow it with 0° angle to y axis. Third layer positioned at 45° angular position to y axis then the sequence continues with first layer. Total size of scaffold was $16.61 \times 16.80 \times 6.60$ mm as seen in Figure 3.1.

Several design variations with different textures and sizes were tested. This was one of the better designs both printable with expected texture details and also supports required pore size value.

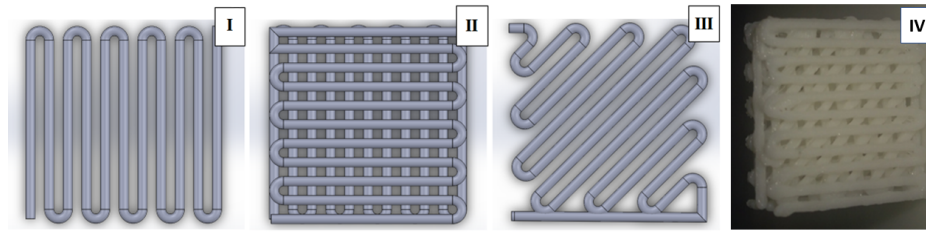


Figure 3.2 I: Layer one, II: Combination of two perpendicular layers, III: 45° third layer and IV: Final printed version of the designed scaffold.

3.2 Material Selection and Application of 3D Printing

The scaffolds were fabricated from filaments of poly(L-lactide) and polycaprolactone blend [PLA/PCL; (70/30 w/w)] by using a 3D printer (Ultimaker 2-Go, Ultimaker, Netherlands) (Fig. 3.3). Blend material could bear combination of biocompatible and mechanical properties of PCL and PLA. It has been reported that 70% to 30% weight percent blending ratio for PLA and PCL showed more favorable properties to prepare scaffolds for bone tissue [13].

Fused Deposition Modelling (FDM), a general bottom-up method, was used for 3D printing. In this approach melted blend polymers by the guidance of nozzle, were assembled layer by layer on top of each other and formed final 3D structure as a whole [6, 39]. Effecting parameters, such as material type, printing speed, material flow rate, table temperature, nozzle temperature, etc, were selected as shown in Table 3.1 [8]. These parameters were the first crucial step for successful 3D construct preparation.

Table 3.1
Optimized 3D printer parameters.

Parameter	Set value
Nozzle Temperature	205°C
Printing Speed	10 mm/s
Table Temperature	60°C
Material Flow Rate	100 mm/s

Combining knowledge from literature, optimum printing temperature for the

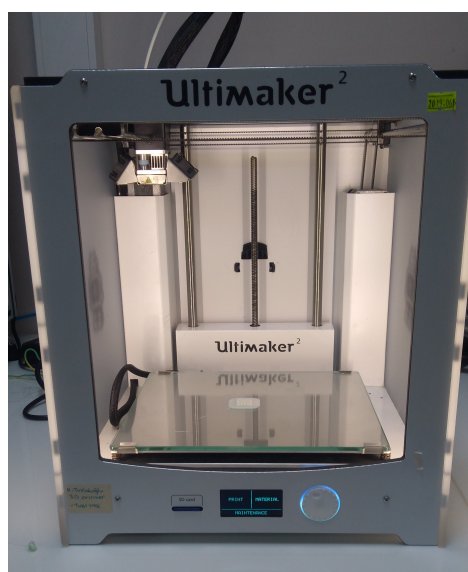


Figure 3.3 Single Extrusion 3D printing machine (Ultimaker 2-Go, Ultimaker, Netherlands).

blend decided as 205°C considering melting temperatures of blend components, printed with fine texture quality and material flow from nozzle with right color and viscosity. From literature, it is known that [PLA/PCL; (70/30 w/w)] blend polymer has melting temperature at 168.40°C. Generally while working with 3D printers increasing temperature to some extent was utilized for achieving more smooth nozzle flow [7, 13]. Since PLA was the dominant component of the blend and has melt process temperature of 210°C as suggested in device data sheet, the process temperature of 205°C was quite reasonable. Elevating the temperature above this point caused flash burn zones on scaffold. And also material flow and printing speed parameters were tweaked to 100 mm/s flow rates and 10 mm/s nozzle travel speed (print speed) of factory settings.

These choices were made to reach smoother surface quality otherwise rough and jagged. Finally template temperature was left as the original setting at 60°C that overall with these settings, there were not any problems about sticking of scaffold to table during printing. Finally template temperature was left as the original setting at 60°C that overall with these settings, there were no problems about texture quality or sticking to table during printing.

3.3 Surface Modification

3.3.1 Alkaline Solution Treatment

Attachment and durability of coated layer is very important for clinical applications and layer have to maintain itself until healing of tissue is completed or until designed time limit is reached. Therefore, pretreatment application before applying biomimetic coating was crucial to improve adhesion strength between apatite layer and scaffold surface. Surface modifications applied prior to the mimetic coating improves the adhesion strength by increasing number of polar groups on the substrate surface [47]. These groups have been found to be acting as favorable nucleating sites for apatite formation in the surface of polymer. There are several strategies to achieve better adhesion strength, such as applying ultraviolet irradiation, hydroxide or hydrochloric acid treatment, the use of bioactive glass particles, etc. Success of these treatment types strictly depend on type of polymer [48, 49].

Herein, NaOH treatment process was chose to modify the surface of the 3D printed scaffolds prior to biomimetic Ca-P coating. Firstly, etching with NaOH were applied to increase bonding initiation points on the surface. The studies have suggested that these locations could increase HA coating stability and rate [4, 8].

Apart from concentration of alkaline solution, etching time was also important parameter for treatment applications. Excess amount of etching could deteriorate the surface of polymer and render its effectiveness altogether. To reach complete penetration of solution into pores, a constant stirring of 100 rpm was applied during the immersion into alkaline solution. After etching, the samples were rinsed with ultra pure water and then dried in an oven at 37 °C. Dried scaffolds were taken and both groups went second step of the surface pretreatment [10].

3.3.2 $CaCl_2$ and K_2HPO_4 Solution Treatment

As mentioned before, in order to increase biomimetic deposition effectiveness many methods have been tested throughout years. Main idea is to increase polar groups at scaffold surface and make surface more appealing for the next phase; Ca-P deposition. In this thesis, 0.2M $CaCl_2$ and 0.2M K_2HPO_4 solutions were also tested for creating initial Ca-P depositions. It has been reported that after NaOH treatment dipping consecutively into these solutions, helps coating quality [12]. These initial points would help HA formation during SBF immersion.

To investigate the effectiveness of $CaCl_2$ and K_2HPO_4 solutions, two samples were first treated with 1M NaOH for 3h and dried at 37°C. Then only one of them was treated with 0.2M $CaCl_2$ and 0.2M K_2HPO_4 solutions consecutively 1 minute for 3 times, followed rinsing and drying. The other sample was not treated with any other solution apart from alkaline treatment in order to clearly see the effects of 0.2M $CaCl_2$ and 0.2M K_2HPO_4 treatment process.

3.4 Preparation of Simulated Body Fluid

During SBF preparation strict guide was followed [37]. First eight materials shown at Table 3.2 were dissolved consecutively in ultra pure water at 36.5°C [37]. To avoid the sudden temperature changes, the solution was placed into a temperature controlled water bath and stirred magnetically at a constant rate.

After all first eight chemicals were dissolved completely, pH of the solution was adjusted by adding Tris and HCl. Tris was added until pH value reaches up to 7.45. Then by lowering with HCl and increasing with Tris, pH value had kept between 7.42-7.45 until all Tris was added to solution. The solution with final pH of 7.4 at 37°C was then left to cool down at room temperature and then stored at +4°C until use [37].

Table 3.2
Simulated Body Fluid Material Content (Sigma Aldrich, Germany) [1].

Materials	Amount
Sodium chloride ($NaCl$)	8.036 g
Sodium of hydrogen carbonate ($NaHCO_3$)	0.352 g
Potassium chloride (KCl)	0.225 g
di-potassium hydrogen phosphate trihydrate (K_2HPO_4)	0.150 g
Magnesium chloride hexahydrate ($MgCl_2 \cdot 6H_2O$)	0.311 g
1M Hydrochloric acid (HCl)	25 ml
Calcium chloride ($CaCl_2$)	0.293 g
Sodium sulfate (Na_2SO_4)	0.072 g
Tris	6.118 g
HCl	15 mL

3.5 Optimization and Application of Biomimetic Coating

Biomimetic coating, like its name suggests, comes from mimicking the human blood plasma with its original ions and temperature to support nucleation of apatite layer on scaffold material. Some methods, such as renewing the ion solution periodically, addition of growth factors or creating constant SBF flow that will mimic active body environment have been suggested to improve the quality of coating [48, 1, 14].



Figure 3.4 Experimental set-up for agitated group.

Pre-treated and dried 3D constructs were placed into falcon tubes and fixed with plastic wires to create stability and give a proper coating chance for all surfaces. Tubes were filled with 1X SBF solution and they were incubated at 37°C for 8, 14 and 21 days. All scaffolds were then removed from the solutions, rinsed with distilled water and left for complete drying at 37°C.

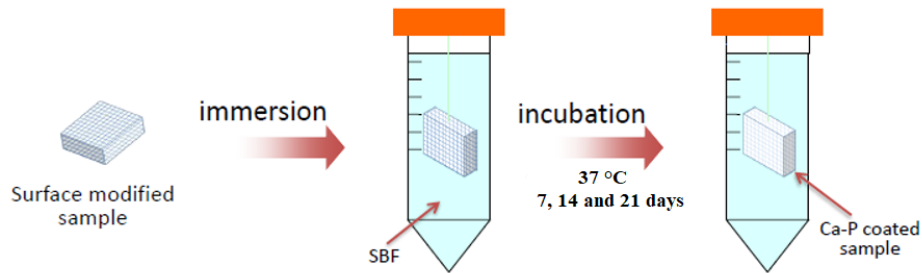


Figure 3.5 Experimental set-up for biomimetic coating.

On top of checking impact of immersion duration difference in coating process, also to investigate the effects of immersion mechanism, three different coating conditions were set for samples; constant agitated group, solution renewed group and lastly still sample group. Agitated samples were placed in shaker-incubator (Thermo scientific) at 100 rpm and at 37°C (Fig. 3.4) . Solution renewed samples were placed in an oven with the same conditions, but differently their medium was renewed with fresh SBF solution in every 3 days. Lastly still sample group was incubated in an oven at 37°C without any special treatment.

3.6 Material Characterization

3.6.1 Scanning Electron Microscopy (SEM)

The top and second layer of coated bone scaffold was visualized by a scanning electron microscope (SEM, XL30 ESEM-FEG, FEI-Philips, Holland) at an accelerated voltage of 20 kV. All samples were sputter coated with gold before the analysis.

3.6.2 Energy-Dispersive X-ray Spectroscopy (EDX)

Electron Dispersive Spectroscopy was also used to determine the presence of Ca and P elements by corresponding individual intensity peaks matched with reference values within the coated layer of the produced scaffold.

3.6.3 X-ray Diffraction Spectroscopy (XRD)

X-ray diffraction technique (XRD) is used to determine the structure, phases, crystal orientation and other structural parameters such as crystallinity, strain, and crystal defects for the crystalline materials. In this thesis, Rigaku D/Max-2200 X-ray diffractometer with monochromatic Cu K α radiation ($\lambda = 1.54 \text{ \AA}$) at 40 kV accelerating voltage and 30 current was utilized for identifying the crystalline phases present. The X-ray patterns of all samples after biomimetic coating were measured in the 2Θ range of 10° and 50° at a scanning rate of $2^\circ/\text{min}$.

3.7 Cell Culture Studies

The cryo-preserved MC3T3 cell line at P12 were removed from liquid nitrogen storage and thawed gently and re-suspended in α -MEM (minimum essential medium, Invitrogen, US) supplemented with 10% fetal bovine serum (FBS, Biochrom AG, Germany) and 1% penicillin/streptomycin (Invitrogen, US). The cell suspension was then transferred into T25 flask and incubated at 37°C in a humidified atmosphere containing 5% CO_2 . The complete medium of the flasks was renewed every 2-3 days until reaching confluency of 85%.

Also cell fixation was applied for 7^{th} and 14^{th} days to preserve cells and tissue components in a life-like state and observe them. Before hand samples were rinsed two times with PBS. Then 750 mL Phosphate buffered saline (PBS) with 10% formaldehyde added on to samples to be left for 1 hour incubation (PBS, tablets, pH 7.4 at 25°C ,

Sigma Aldrich, Taufkirchen, Germany). The samples were then rinse excessively with PBS before subjecting to sequential dehydration in graded series of ethanol. The construct were then dried, mounted onto stubs and sputtered coated with gold before analysing under SEM as described in Section 3.6.1.

3.7.1 Sterilization of Scaffolds

Before cell seeding, all scaffolds were soaked into 70% ethanol for one hour. They were then dried under laminar flow and further sterilized by applying UV light (30 W, 254 nm) per each side for 30 min.

3.7.2 Cell Seeding Process

MC3T3 cells were cultured on top of scaffolds at the density of 5×10^3 by dripping suspension very slowly to let absorption through scaffold pores.

4. RESULTS AND DISCUSSION

4.1 Material Selection

Material selection is one of the crucial steps to design a successful scaffold for bone tissue repair/regeneration. Being similar to biophysical structure of bone and assisting cells just like in their natural environment is the main role of the scaffolds in tissue engineering. Therefore, it is very important to select a proper scaffold material that can easily induce apatite formation on its surface to mimic the inorganic phase of the natural bone. In this thesis, two different materials, namely PLA and its blend with PCL were chosen to produce 3D bone tissue scaffolds. As mentioned before, both PLA and PCL are FDA approved biodegradable polymers and have been extensively used as scaffold material for bone tissue engineering applications mainly due to their acceptable biocompatibility, good mechanical properties and convenient processing. Herein, it was aimed to create a suitable balance by blending two individual polymers to achieve better surface characteristics among the other scaffold properties. Both materials used in 3D printer (Ultimaker 2-Go, Ultimaker, Netherlands) to form scaffolds for bone tissue engineering.

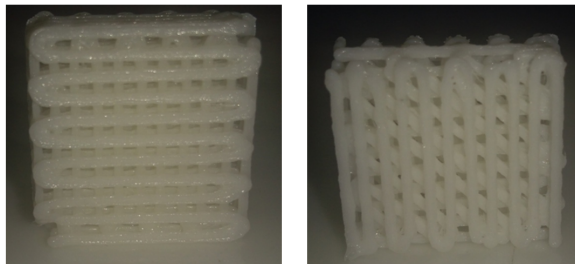


Figure 4.1 Printed final scaffolds.

Both filaments showed excellent performance during printing and formed with expected texture quality as seen in the Figure 4.1. Both scaffold type was subjected under same conditions during pretreatment which involves NaOH treatment (1M, 3h) and 0.2M $CaCl_2$ and K_2HPO_4 solutions then immersion in SBF solution for 14 days.

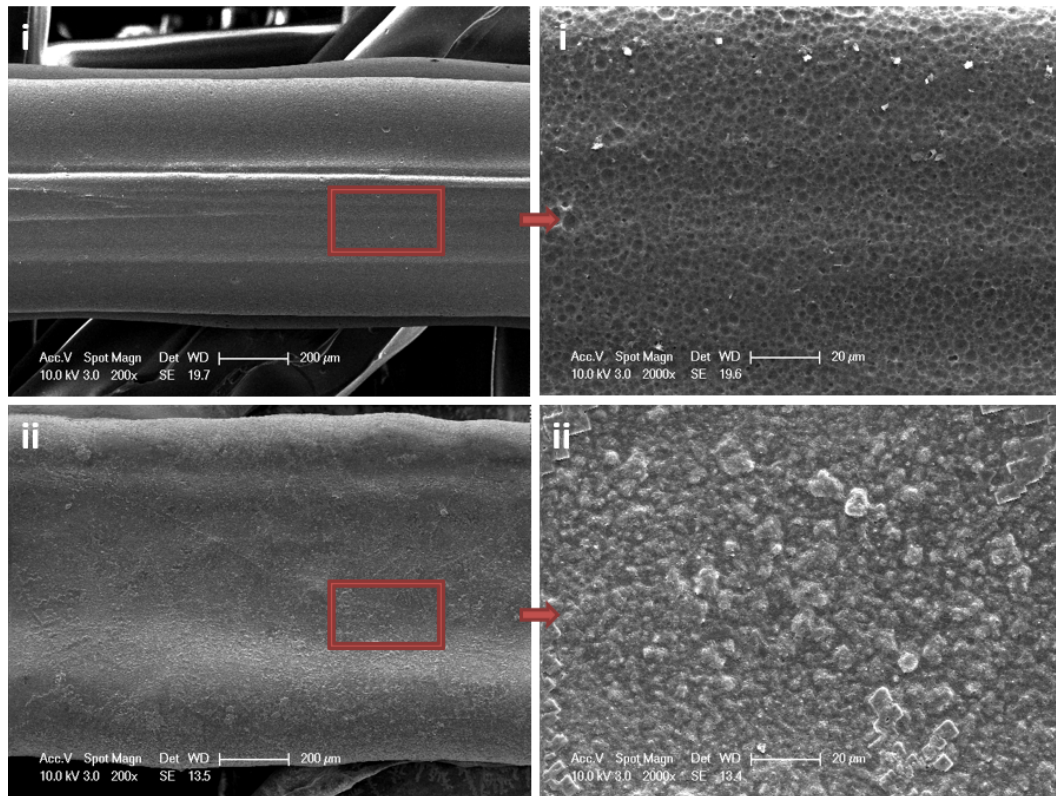


Figure 4.2 After 14 days of immersion, i) PLA scaffold surface, ii) PLA/PCL blend scaffold surface. (Left: 200X, Right side: 2000X magnification).

Comparison between blend material and PLA showed that PCL addition was quite an improvement for coating property of samples. PCL/PLA blend exhibited uniform Ca-P coated surface after immersion in SBF for 14 days which is in close correlation to the previous reports in the literature (Fig. 4.2). Coated surface after 14 days in SBF solution described in literature [17, 10, 33]. Even though Ca-P layer clearly visible at increased magnification of scaffolds made of PLA/PCL blend, from Figure 4.2, PLA scaffold surface did not show any sign of Ca-P precipitation, but few salt crystals were observed on the surface. PLA sample surface had only groves that is very similar to the literature images from etched PLA surface [13, 47].

Further more, as Kokubo informed, the Ca-P formation is critical in early stages and layers develop from those early initiation points [37]. That being said increasing immersion duration would not benefit Ca-P coating capability of PLA sample. Thus, these preliminary test showed that PLA/PCL blends had ability to induce bone-like apatite coating and the further experiments were performed using this blend.

It is also important to note that for some filaments made of common materials, such as PLA and ABS, the printing conditions are readily available in data sheets for each type of printer. However, as we used a special filament made of PLA/PCL blend it was necessary to determine the optimum printing parameters for FDM printing method.

4.2 Surface Modification

4.2.1 Effects of Alkaline Solution

In order to obtain the most convenient surface for biomimetic coating, different concentration of alkaline solution and immersion time were tested as presented Table 4.1. One variable was always kept constant when the other was changed. The lowest and highest concentrations for NaOH were 1M and 3M, respectively. It was observed that not enough etching occurred below 1M NaOH concentration, where the NaOH concentrations higher than 3M caused damages on the material. Thus, these two concentration values were chosen for the optimization of surface treatment parameters.

Table 4.1
Surface Treatment Groups.

Group Label	<i>NaOH</i> Concentration	Immersion Duration
A	1M	1h
B	3M	3h
C	1M	3h
D	3M	1h

Samples treated with different conditions were investigated under SEM and results were showed that changes on the concentration of alkaline solution and duration of dipping directly affected the amount of Ca-P layer formed on the surface of the scaffolds (Fig. 4.3). As it was clearly seen in SEM micrographs, the largest layer of Ca-P was formed on the surface of the samples treated with 1M NaOH for 3h. According

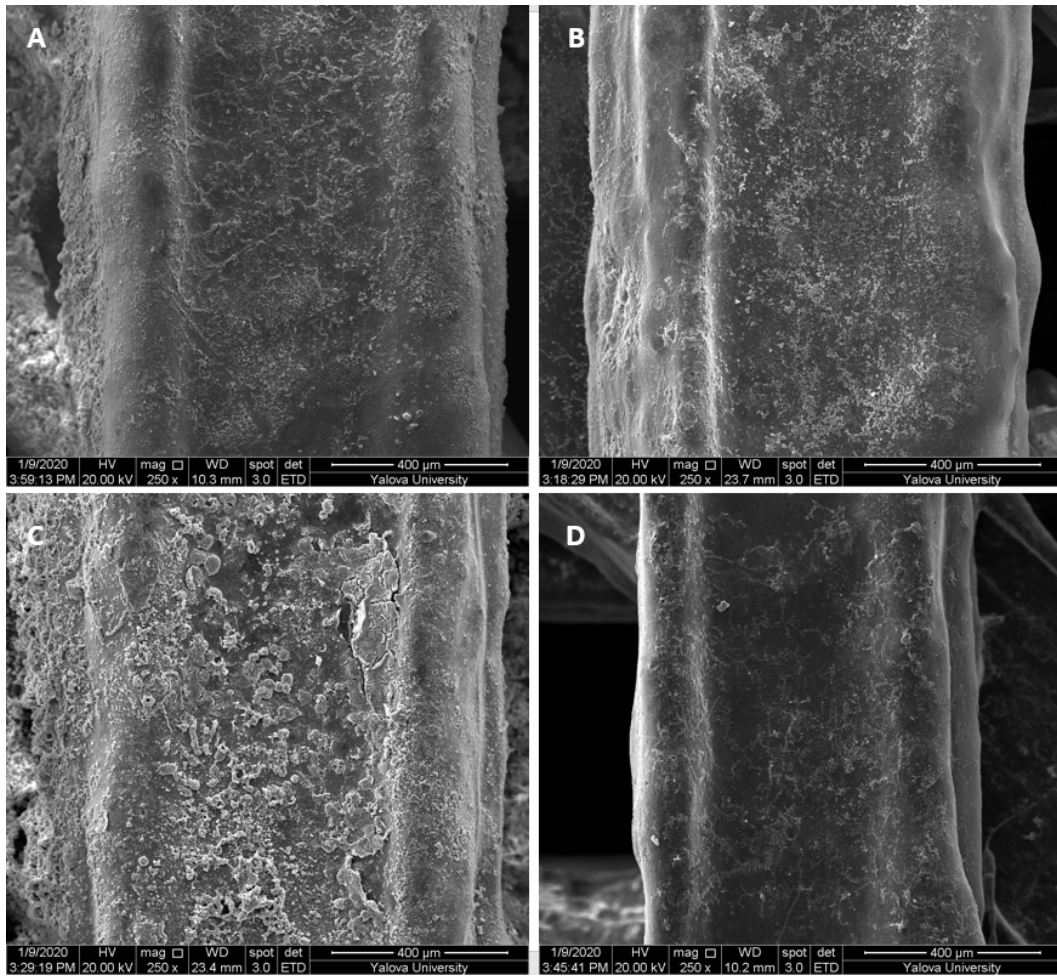


Figure 4.3 SEM images of PCL/PLA blend scaffolds after application of alkaline and $CaCl_2$ and K_2HPO_4 solutions with varying duration; A)1M alkaline treatment for 1h. B)3M alkaline treatment for 3h. C)1M alkaline treatment for 3h. D)3M alkaline treatment for 1h (250X).

to the study, it could be said that limited immersion time and concentration both affected A sample's coating quality and weight gain poorly that surface was bearing minimum amount of Ca-P formation [10]. In both cases for B and D group, alkaline treatment with 3M solution is not improved the coating quality.

Overall, from SEM results, it could be said that the best option for surface treatment of the produced 3D scaffolds was as in option C which involves etching 3 hours in 1M NaOH solution. Initial points that created could be further utilized with additional solution treatments like 0.2M $CaCl_2$ and K_2HPO_4 solutions [12].

4.2.2 Effects of $CaCl_2$ and K_2HPO_4 Solutions

After initial surface modification with NaOH solution, the scaffolds were further treated by dipping into solutions riched with Ca and/or P ions. As alkaline treatment introduce carboxylate groups on the surfaces by causing hydrolytic chain scission of the ester group of polymers, Ca and P ions could adsorb better on the surface and can induce nuclei formation during immersion in SBF.

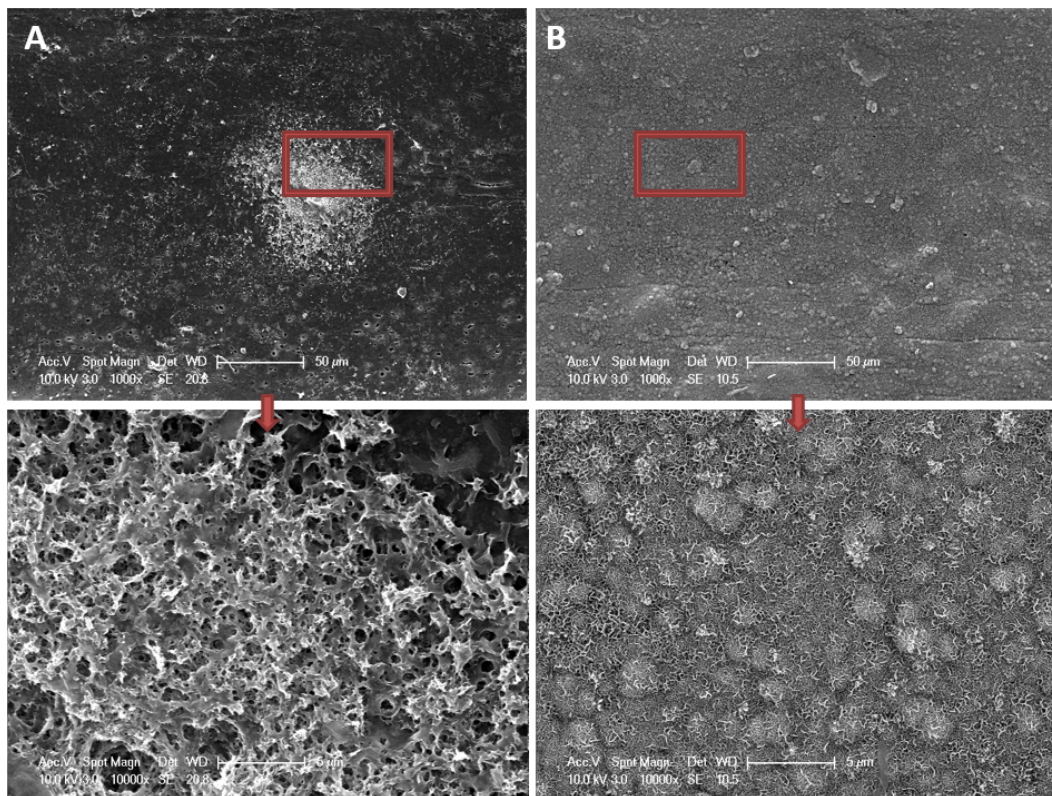


Figure 4.4 SEM images of PCL/PLA scaffold sample surface without solution treatment (A) and same sample with surface treatment by consecutive solution dipping (B) (Upper images: 1000x, lower images: 10.000x magnification).

Two groups were separated according to their solution treatment. After initial 1M NaOH treatment for 3h, group A was treated with 0.2 M $CaCl_2$ and K_2HPO_4 solutions. From SEM images, results clearly showed that creating initiation points for HA structures had benefits for their coating effectiveness and coated layer spread. From Figure 4.4, untreated sample A had a very limited coated regions. They were depositing on top of each other and there was limited spreading. It was creating highly clustered formations. Magnification to these clusters were proving that they

were actually HA depositions but in a very small and limited areas. On the other hand $CaCl_2$ and K_2HPO_4 treated sample was showing continuous wide deposition of HA all over the scaffold. Increased magnification on B sample proved the very characteristic formation of HA structures [17, 1]. This experiment proved that treatment with $CaCl_2$ and K_2HPO_4 solutions improved the amount of Ca-P deposited layer.

4.3 Effects of Simulated Body Fluid on Coating Quality under Continuous Agitation and Periodic Solution Renewing

To investigate the effects of different immersion conditions for Ca-P coating, three distinct groups were determined. Although all groups were incubated in SBF solution (50ml) at 37°C, agitated group was subjected to constant agitation (100 rpm) in the shaker incubator (Thermo Scientific MaxQ 4000). For renewed group's SBF solution was renewed every third day. Finally still group was incubated in an incubator at 37°C without any special treatment. On top of that, to determine the effect of immersion time, three different time points, 8th, 14th, and 21th days, were set for all groups.

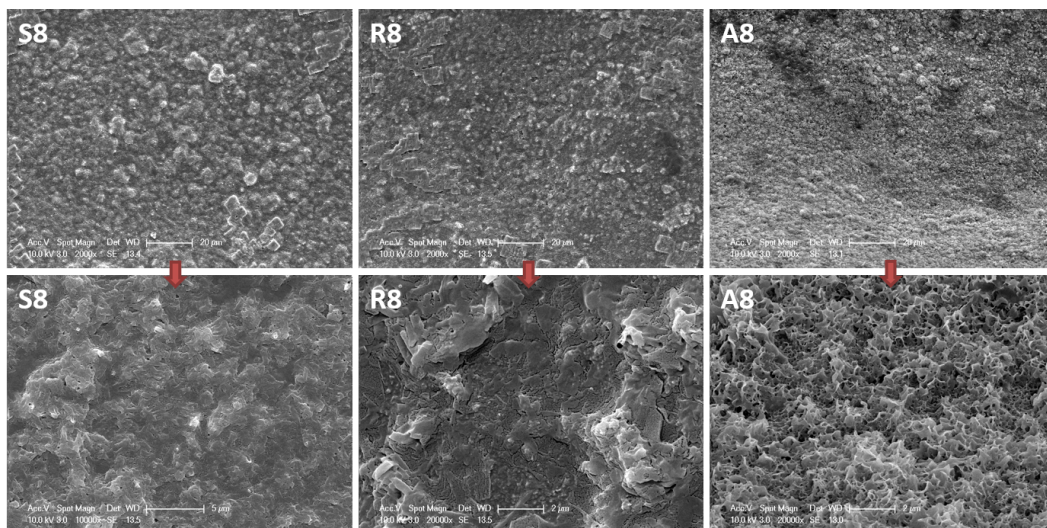


Figure 4.5 8th day SEM images. S8: Still group, R8: Solution Renewed group, A8: Agitated group (Upper images: 2000x, bottom images: 20.000x magnification).

SEM images exhibited the clear difference between the groups. For all three

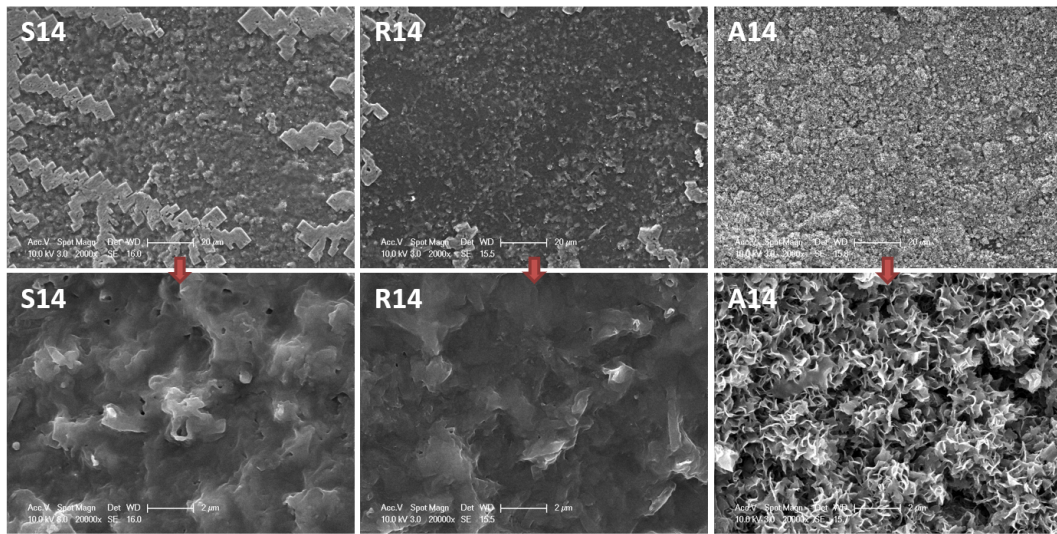


Figure 4.6 14th day SEM images. S14: Still group, R14: Solution Renewed group, A14: Agitated group (Upper images: 2000x, bottom images: 20.000x magnification).

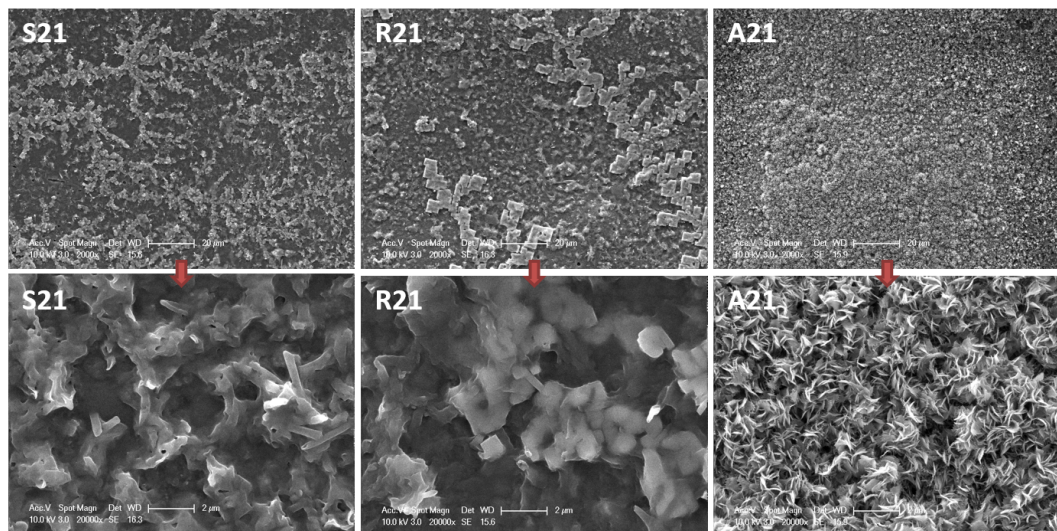


Figure 4.7 21th day SEM images. S21: Still group, R21: Solution Renewed group, A21: Agitated group (Upper images: 2000x, bottom images: 20.000x magnification).

groups apatite layer formation was visible, but especially agitated samples were clearly showing characteristic pattern of HA across the surface [49, 1]. These patterns became more clear with the advancing duration from 8th day to 21th (Fig. 4.5 and Fig. 4.7). On the other hand, deposition characteristics of other two groups were quiet different than agitated samples that even at 2000x magnification, difference between deposition types were clearly visible. Between agitated and still group, still group samples had smoother surface (Fig. 4.5). Even with increased duration in SBF solution, the characteristic look of HA, such as in agitated samples, was not obtained. Interestingly, there was rather

similarity between solution renewed and still groups in terms of apatite topography. Under 20.000x magnification these two groups almost inseparable unlike in the case of agitated groups. Between S21, R21 and A21 this particular difference could be clearly detected. Thus, it could be deduced that agitation mechanism for biomimetic coating during SBF immersion had a significant effect on Ca-P formation characteristic.

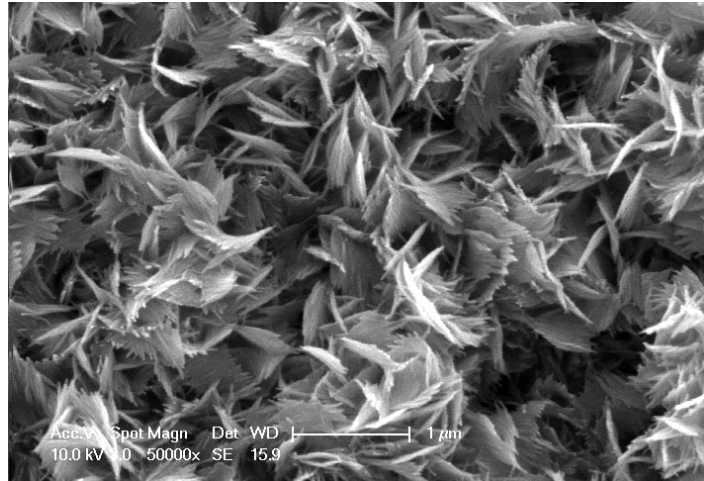


Figure 4.8 SEM image of PCL/PLA Scaffold that constantly agitated during 21 days SBF immersion (50.000x magnification).

Furthermore, surface of the agitated samples were exhibited completely different morphology after coating than those of other groups. There was noticeable change on the morphology of formed CA-P layer on surface between 8th, 14th and 21th days of immersion.

Needle-like formation of deposited Ca-P structure was clearly increasing with increasing immersion time. The reason behind that could be immersion for 21 days, longest immersion time, warped the known formation of Ca-P into more needle-like structure (Fig. 4.7). More detailed Figure 4.8 with 50.000X magnification clearly showed how different the formation became at 21th day rather than 8th day agitated sample.

Interior structure of the 3D scaffold had to be in the same manner with its surface. Porous structure of our design had benefits on penetration of SBF solution thus complete inside-out coating of scaffold. In Figure 4.9, it was clear that even second

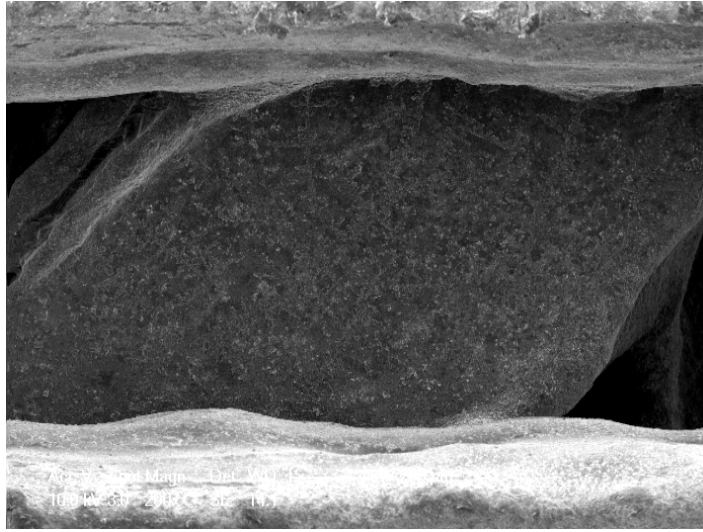


Figure 4.9 SEM image of interior layer of PCL/PLA scaffold after 14 days of SBF immersion (200x magnification).

layer of scaffold was uniformly coated with Ca-P structure. This would allow cells to propagate interiors of scaffold, attach to surface and create 3D tissue structure.

4.4 EDX Analysis

EDX analysis of all three groups immersed in SBF under different conditions. Separate distinct intensity peaks measured at 0.277, 0.535, 2.013, 3.690 keV according to their excitation of atomic energy level. Control group being the plain untreated PLA/PCL blend the results were same with literature that respectively 0.277 and 0.535 keV values corresponding to Carbon (C) and Oxygen (O) peaks [50, 51, 52] (Fig. 4.10). These peaks became constant for all graphs because of PLA/PCL blend being base material of all scaffolds.

All three groups represented here showed very similar trend among them that after 8 days of immersion in SBF solution led phosphate (P) (2.013 keV) and calcium (Ca) (3.690 keV) peaks formation in EDX analysis for all groups. Then increasing duration of these immersions, as expected, gradually enhanced the intensities of these mentioned peaks reaching the highest intensities at 21th day samples [14, 37].

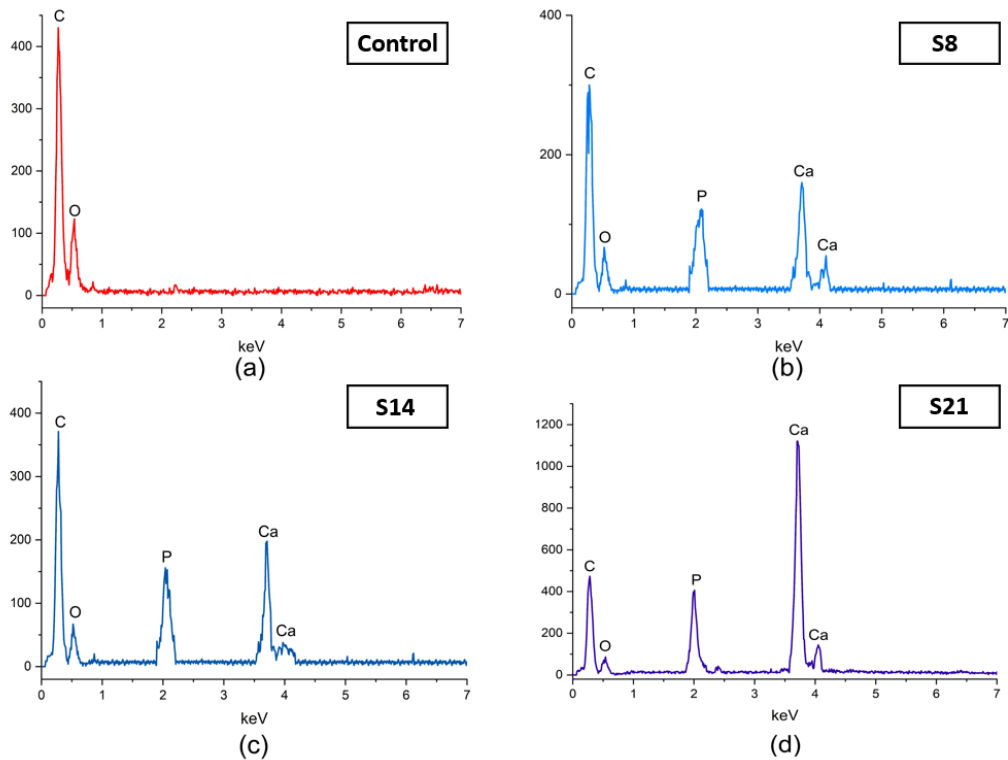


Figure 4.10 EDX graphs for still samples for 8th (S8), 14th (S14) and 21th (S21) days.

Apart from other groups as seen in the Figure 4.11, renewed group was showing similar intensities around 600-700 all for 8, 14 and 21 days immersed samples. Intensities of Ca and P elements for still and agitated groups were around 200-300 at 8th and 14th days but these values increased to 1100-1200 at 21th day results. The reason behind that could be renewing solution was replenishing the consumed calcium and phosphate ions in the fluid and introducing new calcium and phosphate ions into system thus leading to fast biomimetic reaction resulting as measurement of intense peaks at 8th day [48, 14]. Then after initial layer formation there were only small differences in terms of intensities in the following days of the solution renewed samples. Seeing calcium and phosphate peaks at every group also proved that [PLA/PCL; (70/30 w/w)] blend scaffold could be coated with Ca-P layer with applied surface modifications from this thesis.

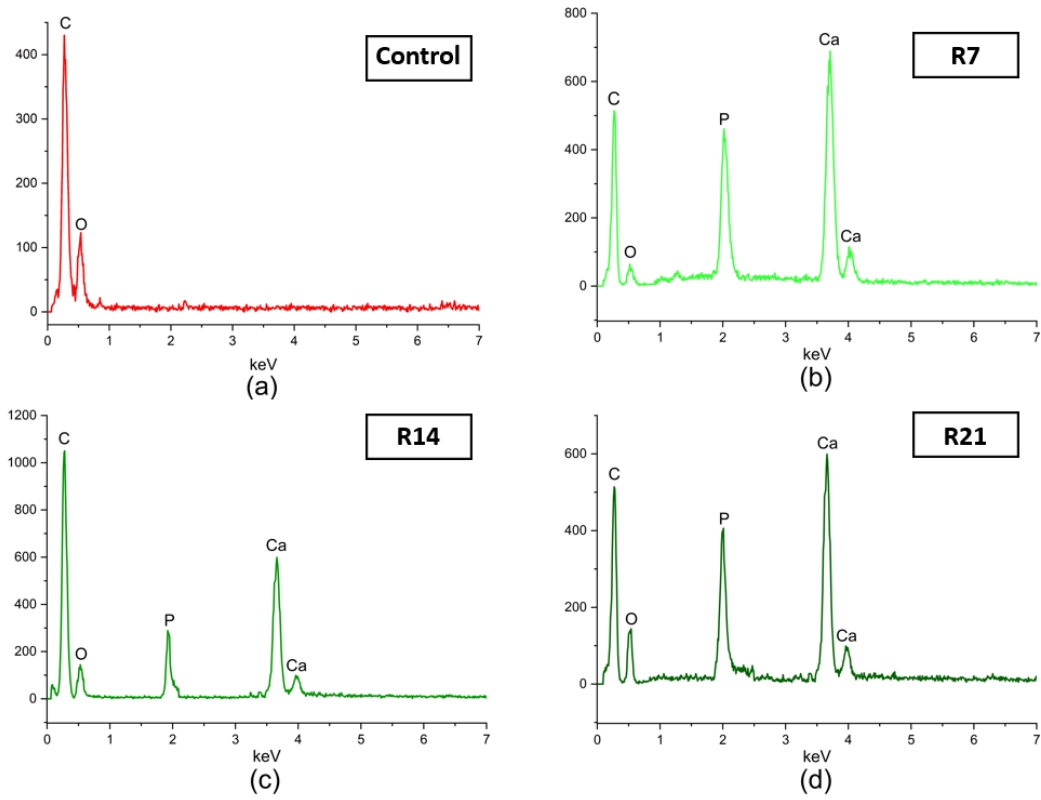


Figure 4.11 EDX graphs for solution renewed samples for 8th (R8), 14th (R14) and 21th (R21) days.

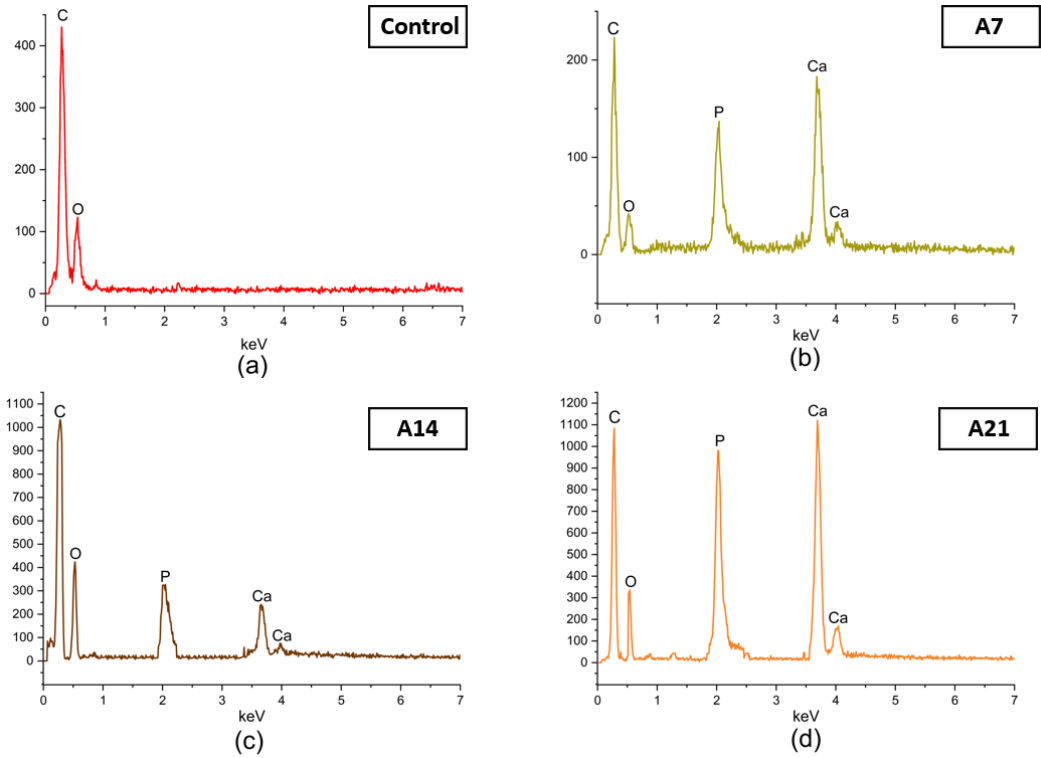


Figure 4.12 EDX graphs for solution agitated samples for 8th (A8), 14th (A14) and 21th (A21) days.

4.5 XRD Analysis

Figure 4.13 shows the XRD patterns of all the samples immersed in SBF under different conditions. The distinct diffraction peaks near at 2θ of 23° , 25° , and 29° observed in all samples corresponding to semi-crystalline PCL [53]. A broad reflection peaks near to 2θ of 16° was associated to the crystal lattice (200)/(110) of α -type of PLA [54]. After immersion in SBF for 14 days, the presence of apatite with a diffraction peak at 2θ angle of 32° and 46° appeared in the XRD patterns of the scaffolds (Fig. 4.15). As the coating time was increased, the intensity of the apatite peaks also increased gradually indicating more deposition of the apatite crystals (Fig. 4.17, 4.19, 4.18). Though these peaks were barely visible at day 8, the region around apatite peaks were smoother than that on control, which indicates the apatite formation (Fig. 4.14). This fact might be due to the formation of amorphous apatite predominantly on the scaffold surfaces in the first days of immersion [38].

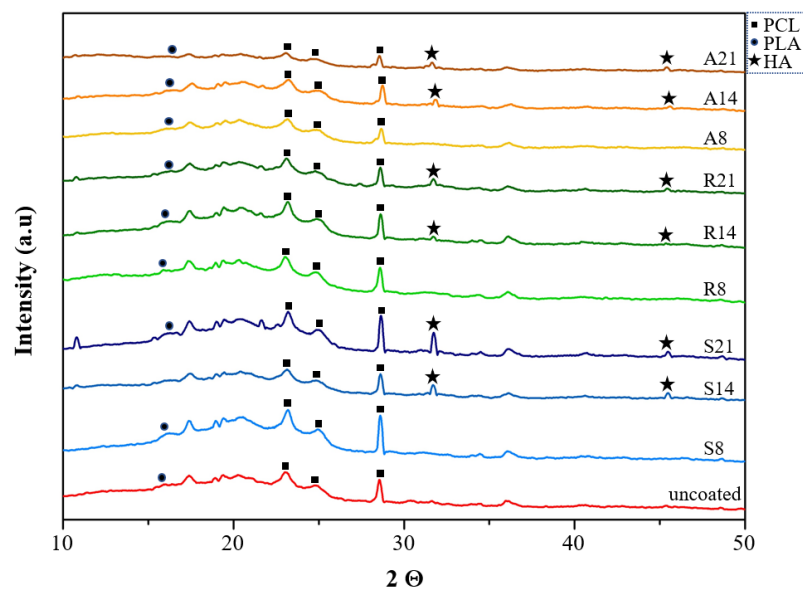


Figure 4.13 XRD spectra of all HA coated sample groups according to their SBF immersion conditions and duration times.

It was also observed that the immersion conditions had also influence on the deposition of apatite crystals as presented in Figure 4.13. Intensity of apatite-related peaks were higher at the XRD patterns of still samples than that of renewed and agitated ones. The reason for that could be as first stated in 1997 by Kokubo then

after proved with many following researches that concept of hydroxyapatite formation strictly depends on the initial nucleation stage and conditions of the area where calcium free ions must attach to surface before completing HA crystallization [37, 40, 18, 55]. Simply changing substrate surface, deposition rate or temperature could affect HA deposition [56]. On top of that, it is known that X-Ray diffraction peaks and their intensities depends on elemental composition and preparation conditions. During the preparation process, layer formation may take a certain direction for growing which is accepted as preferred orientation type of that material. From this information, the reason behind higher peak intensities at still samples than other groups, could be explained as both frequent solution renewing and 100 rpm agitation was deterring from preferred formation orientation of HA layer. Nonetheless all three groups successfully showed characteristic HA peaks at the end of their 21th day SBF immersion as represented in Figure 4.16.

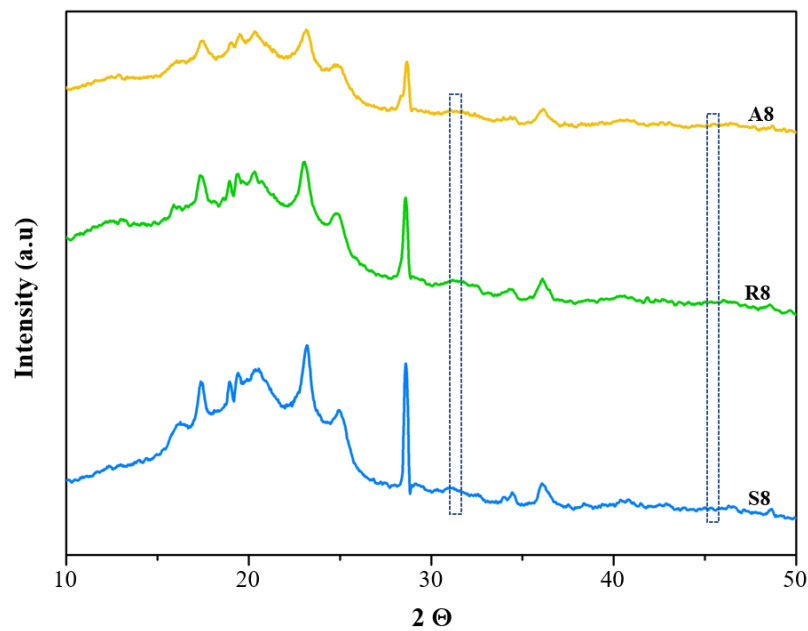


Figure 4.14 XRD spectra of three sample groups after 8 days of SBF immersion.

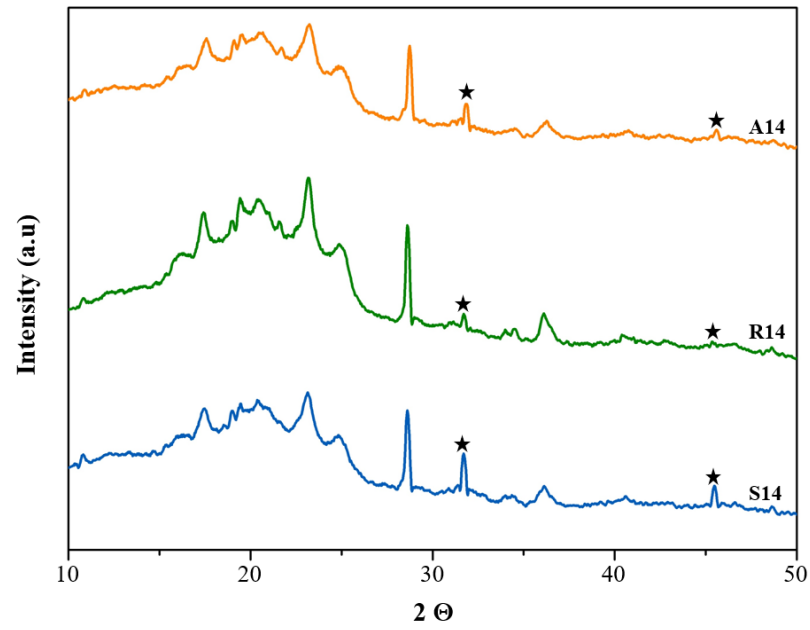


Figure 4.15 XRD spectra of three sample groups after 14 days of SBF immersion.

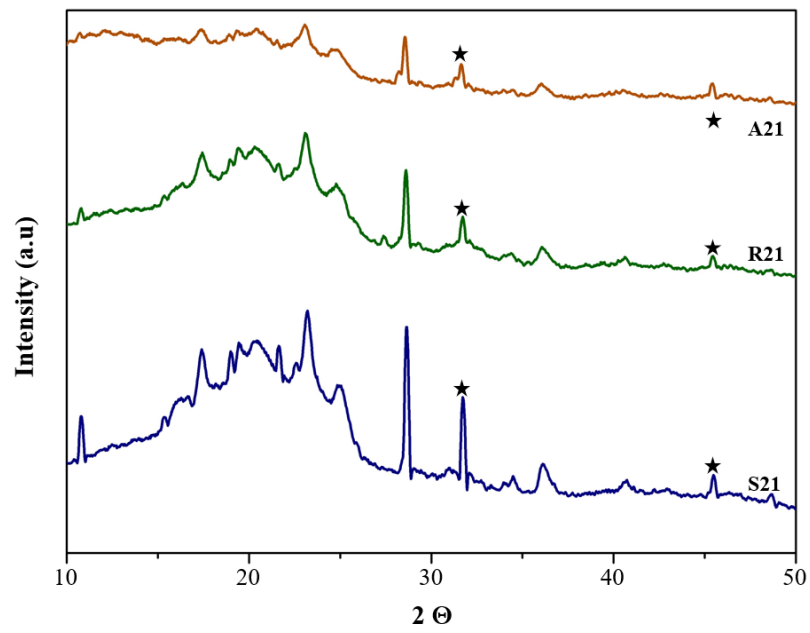


Figure 4.16 XRD spectra of three sample groups after 21 days of SBF immersion.

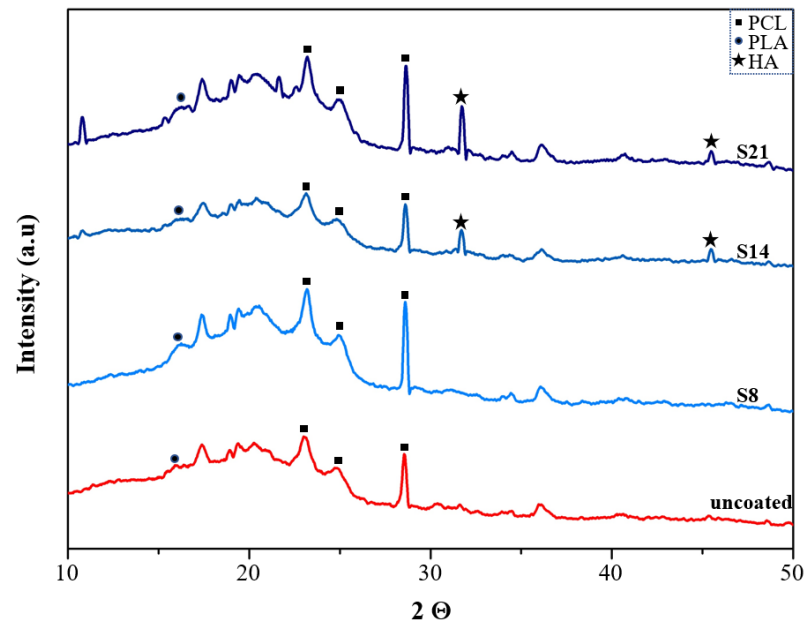


Figure 4.17 XRD spectra of Still sample groups according their duration in SBF solution.

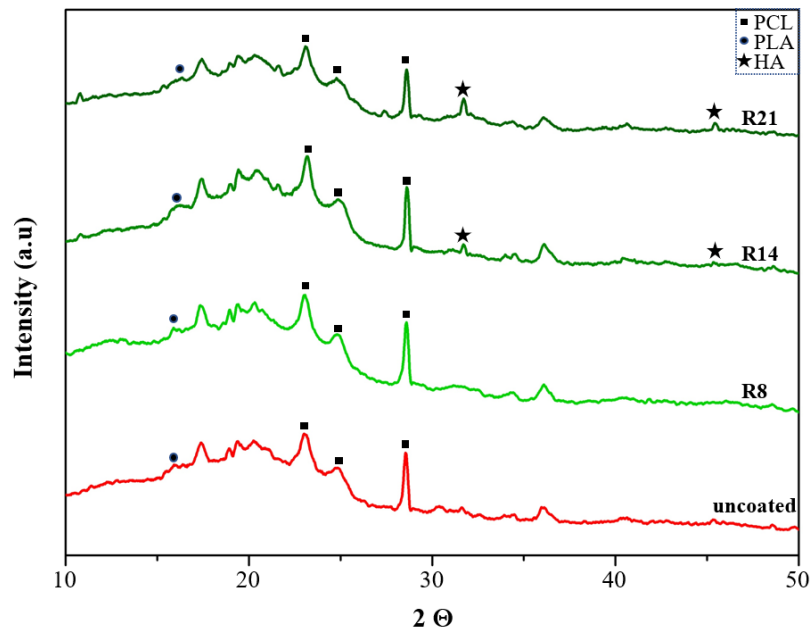


Figure 4.18 XRD spectra of Renewed sample groups according their duration in SBF solution.

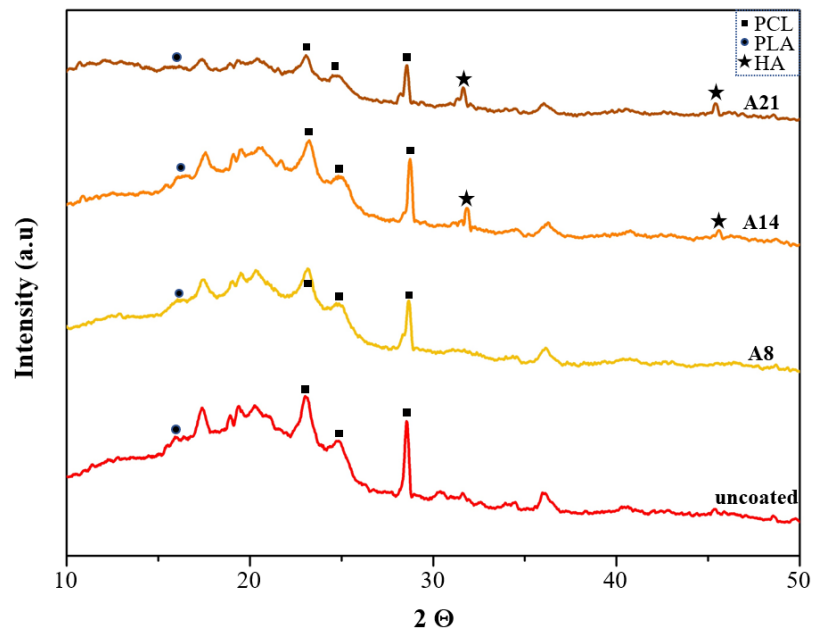


Figure 4.19 XRD spectra of Agitated sample groups according to their duration in SBF solution.

4.6 *InVitro* Cell Culture Studies

Preliminary studies were conducted to investigate the adhesion of osteoblast like cells on the coated surfaces. All scaffolds were treated with previously optimized pretreatment procedures (alkaline etching then $CaCl_2$ and K_2HPO_4 solutions treatment) and then immersed in SBF solution under agitated group parameters (100 rpm, $36^\circ C$). The results from Figure 4.20 showed that there were clear cell attachments on Ca-P coated surface. On the other hand, samples without Ca-P layer were showing just few attached cells on the surface.

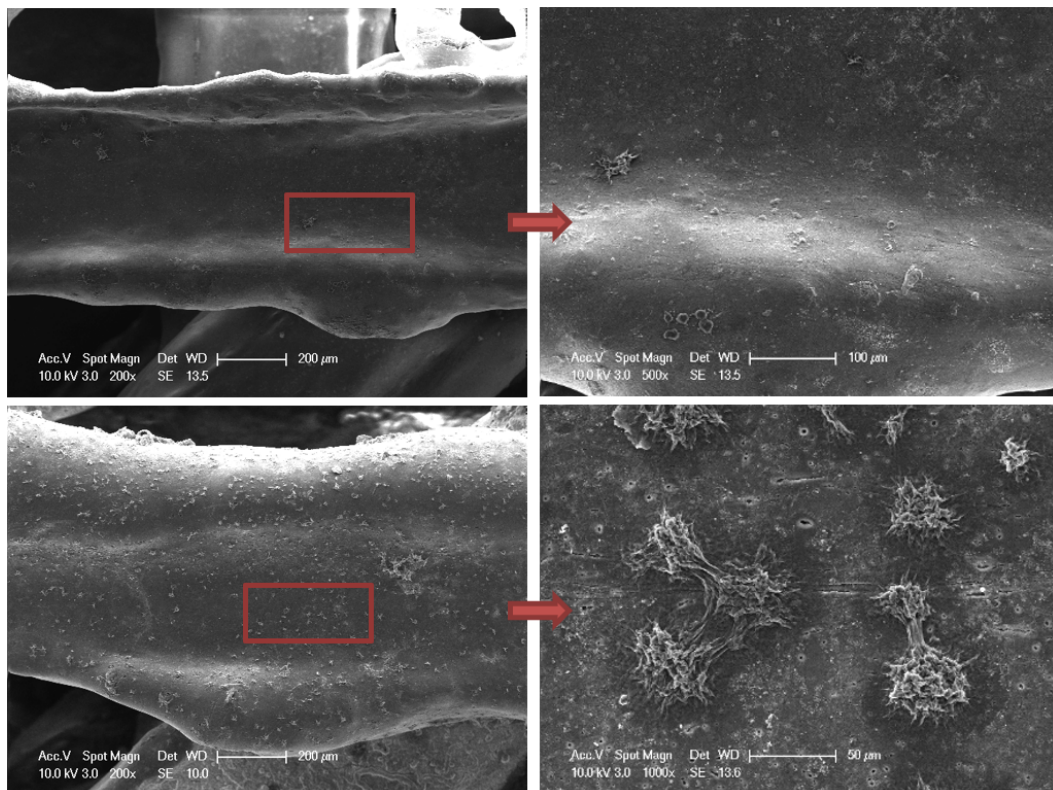


Figure 4.20 14 day SEM images (Upper images; without coating, lower images; with Ca-P coating on the surface).

The reason behind could be the changes in the surface chemistry of the scaffolds. It is well-known that the surface chemistry and the topography can directly affect the osteoblast like cell response and determine cell attachment through binding protein, ligands and integrins. To support that, Figure 4.21 with 10.000x magnification was utilized to see clear attachment of cells onto the Ca-P deposited surface.

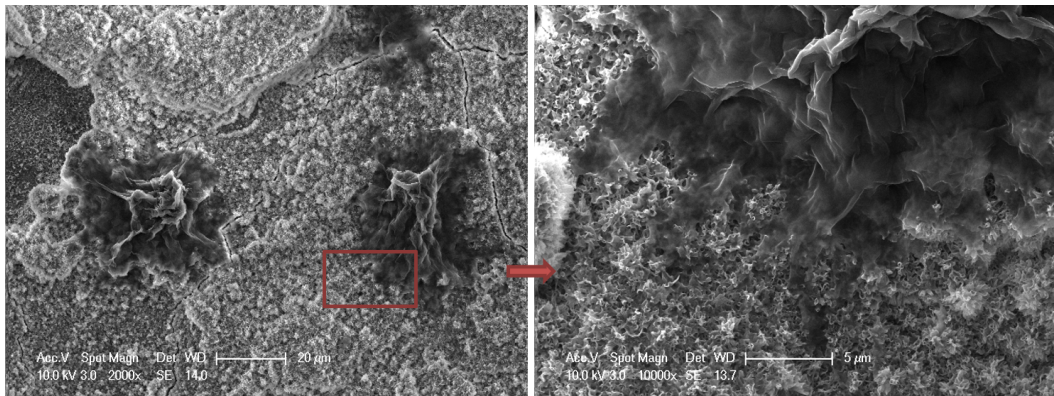


Figure 4.21 14 day SEM images of cells attached to Ca-P coated surface.

5. CONCLUSION

In this study;

- Blend [PLA/PCL; (70/30 w/w)] polymer was utilized and successfully optimized for detailed scaffold printing with 3D printer. And it was proved with SEM results that blend polymer was better candidate for biomimetic Ca-P coating method.
- Pretreatment conditions were investigated and as a result scaffolds were pretreated with 1M NaOH alkaline solution for 3 hours and then following to that 0.2M $CaCl_2$ and 0.2M K_2HPO_4 solutions were applied for 3x1 minute to reach most dense and well formed Ca-P apatite layer on scaffold surface which were closely investigated and confirmed with EDX and XRD analysis.
- Three distinct groups for SBF immersion were tested for biomimetic Ca-P apatite layer coating approach and despite EDX results represents clear Ca-P formation for all groups, from SEM results agitated group showed more distinct needle-like formation than other immersion methods.
- Cell culture studies proved that Ca-P layer enhance attachment of cells on to the scaffold surface rather than uncoated scaffolds.

REFERENCES

1. Tuzlakoglu, K., and R. L. Reis, "Formation of bone-like apatite layer on chitosan fiber mesh scaffolds by a biomimetic spraying process," *Journal of Materials Science: Materials in Medicine*, Vol. 18, pp. 1279–1286, Jul 2007.
2. Chen, Y., A. F. Mak, M. Wang, J. Li, and M. S. Wong, "Plla scaffolds with biomimetic apatite coating and biomimetic apatite/collagen composite coating to enhance osteoblast-like cells attachment and activity," *Surface and Coatings Technology*, Vol. 201, pp. 575–580, Oct 2006.
3. Deplaine, H., M. Lebourg, P. Ripalda, A. Vidaurre, P. Sanz-Ramos, G. Mora, F. Prosper, I. Ochoa, M. Doblaré, J. L. Gomez Ribelles, I. Izal-Azcárate, and G. Gallego Ferrer, "Biomimetic hydroxyapatite coating on pore walls improves osteointegration of poly(l-lactic acid) scaffolds," *Journal of Biomedical Materials Research - Part B Applied Biomaterials*, Vol. 101 B, pp. 173–186, Jan 2013.
4. Shin, K., T. Acri, S. Geary, and A. K. Salem, *Biomimetic Mineralization of Biomaterials Using Simulated Body Fluids for Bone Tissue Engineering and Regenerative Medicine*, Mary Ann Liebert Inc., 1991.
5. Polo-Corrales, L., M. Latorre-Esteves, and J. E. Ramirez-Vick, "Scaffold design for bone regeneration," *Nanoscience and Nanotechnology*, Vol. 14, pp. 15–56, Jan 2014.
6. Arul, K. T., E. Manikandan, and R. Ladchumananandasivam, "Polymer-based calcium phosphate scaffolds for tissue engineering applications," in *Nanoarchitectonics in Biomedicine*, pp. 585–618, Elsevier, 2019.
7. Okamoto, M., "The role of scaffolds in tissue engineering," in *Handbook of Tissue Engineering Scaffolds: Volume One*, pp. 23–49, Elsevier, 2019.
8. Derakhshanfar, S., R. Mbeleck, K. Xu, X. Zhang, W. Zhong, and M. Xing, "3d bioprinting for biomedical devices and tissue engineering: A review of recent trends and advances," *Bioactive Materials*, Vol. 3, no. 2, pp. 144–156, 2018.
9. Matai, I., G. Kaur, A. Seyedsalehi, A. McClinton, and C. T. Laurencin, "Progress in 3d bioprinting technology for tissue/organ regenerative engineering," *Biomaterials*, Vol. 226, pp. 119–536, Sep 2020.
10. Kramer, E., B. Kunkemoeller, and M. Wei, "Evaluation of alkaline pre-treatment of plla fibers for biomimetic hydroxyapatite coating," *Surface and Coatings Technology*, Vol. 244, pp. 23–28, Mar 2014.
11. Howard, D., L. D. BATTERY, K. M. Shakesheff, and S. J. Roberts, "Tissue engineering: Strategies, stem cells and scaffolds," *Current Opinion in Biomedical Engineering*, Vol. 213, no. 1, pp. 66–72, 2008.
12. Yokoyama, Y., A. Oyane, and A. Ito, "Biomimetic coating of an apatite layer on poly(l-lactic acid); improvement of adhesive strength of the coating," *Journal of Materials Science: Materials in Medicine*, Vol. 18, pp. 1727–1734, Sep 2007.
13. Matta, A., R. U. Rao, K. Suman, and V. Rambabu, "Preparation and characterization of biodegradable pla/pcl polymeric blends," *Procedia Materials Science*, Vol. 6, pp. 1266–1270, 2014.

14. Oliveira, A. L., P. B. Malafaya, S. A. Costa, R. A. Sousa, and R. L. Reis, "Micro-computed tomography (μ -ct) as a potential tool to assess the effect of dynamic coating routes on the formation of biomimetic apatite layers on 3d-plotted biodegradable polymeric scaffolds," *Journal of Materials Science: Materials in Medicine*, Vol. 18, pp. 211–223, Feb 2007.
15. Turon, P., L. J. del Valle, C. Alemán, and J. Puiggali, "Grafting of hydroxyapatite for biomedical applications," in *Biopolymer Grafting: Applications*, pp. 45–80, Elsevier, 2018.
16. Chou, L., B. Marek, and W. R. Wagner, "Effects of hydroxylapatite coating crystallinity on biosolubility, cell attachment efficiency and proliferation in vitro," *Biomaterials*, Vol. 20, pp. 977–985, Dec 1999.
17. Peng, F., M. T. Shaw, J. R. Olson, and M. Wei, "Influence of surface treatment and biomimetic hydroxyapatite coating on the mechanical properties of hydroxyapatite/poly(l-lactic acid) fibers," *Journal of Biomaterials Applications*, Vol. 27, pp. 641–649, Feb 2013.
18. Prakasam, M., J. Locs, K. Salma-Ancane, D. Loca, A. Largeteau, and L. Berzina-Cimdina, "Fabrication, properties and applications of dense hydroxyapatite: A review," *Journal of Functional Biomaterials*, Vol. 6, no. 4, pp. 1099–1140, 2015.
19. Ellingson, K. T., and J. P. Galassi, "Testing two theoretical explanations for the attraction-enhancing effects of self-disclosure," *Journal of Counseling & Development*, Vol. 73, no. 5, pp. 535–541, 1995.
20. Harada, S. I., and G. A. Rodan, "Control of osteoblast function and regulation of bone mass," *Nature*, Vol. 423, no. 6937, pp. 349–355, 2003.
21. Liebschner, M. A., "Biomechanical considerations of animal models used in tissue engineering of bone," *Biomaterials*, Vol. 25, no. 9, pp. 1697–1714, 2004.
22. Hamed, E., Y. Lee, and I. Jasiuk, "Multiscale modeling of elastic properties of cortical bone," *Acta Mechanica*, Vol. 213, no. 1-2, pp. 131–154, 2010.
23. Roohani-Esfahani, S. I., P. Newman, and H. Zreiqat, "Development of nanocomposites for bone grafting," *Composites Science and Technology*, Vol. 65, no. 15-16, pp. 2385–2406, 2005.
24. Nakashima, T., and H. Takayanagi, "New regulation mechanisms of osteoclast differentiation," *Annals of the New York Academy of Sciences*, Vol. 1240, pp. 13–18, 2011.
25. LaStayo, P. C., K. M. Winters, and M. Hardy, "Fracture healing: Bone healing, fracture management, and current concepts related to the hand," *Journal of Hand Therapy*, Vol. 16, no. 2, pp. 81–93, 2003.
26. Sarkar, M. R., N. Wachter, P. Patka, and L. Kinzl, "First histological observations on the incorporation of a novel calcium phosphate bone substitute material in human cancellous bone," *Journal of Biomedical Materials Research*, Vol. 58, no. 3, pp. 329–334, 2001.
27. Sanchez Garces, M. A., J. Escoda-Francoli, and C. Gay-Esco, "Implant complications," *Implant Dentistry - The Most Promising Discipline of Dentistry*, 2011.
28. Ronca, D., F. Langella, M. Chierchia, U. D'Amora, T. Russo, M. Domingos, A. Gloria, P. Bartolo, and L. Ambrosio, "Bone tissue engineering: 3d pcl-based nanocomposite scaffolds with tailored properties," *Procedia CIRP*, Vol. 49, pp. 51–54, 2016.

29. Mirón, V., S. Ferrándiz, D. Juárez, and A. Mengual, "Manufacturing and characterization of 3d printer filament using tailoring materials," *PLoS ONE*, Vol. 13, pp. 888–894, 2017.
30. Ragunathan, S., G. Govindasamy, D. Raghul, M. Karuppaswamy, and R. Vijayachandrasekaran, "Hydroxyapatite reinforced natural polymer scaffold for bone tissue regeneration," *Materials Today: Proceedings*, 2019.
31. Chan, B. P., and K. W. Leong, "Scaffolding in tissue engineering: General approaches and tissue-specific considerations," *European Spine Journal*, Vol. 17, 2008.
32. LeGeros, R. Z., "Properties of osteoconductive biomaterials: Calcium phosphates," *Biomaterials*, no. 395, pp. 81–98, 2002.
33. Mondal, S., T. P. Nguyen, V. H. Pham, G. Hoang, P. Manivasagan, M. H. Kim, S. Y. Nam, and J. Oh, "Hydroxyapatite nano bioceramics optimized 3d printed poly lactic acid scaffold for bone tissue engineering application," *Ceramics International*, pp. 1–13, Jul 2019.
34. Hassanajili, S., A. Karami-Pour, A. Oryan, and T. Talaei-Khozani, "Preparation and characterization of pla/pcl/ha composite scaffolds using indirect 3d printing for bone tissue engineering," *Materials Science and Engineering C*, Vol. 104, pp. 1221–1227, Jul 2019.
35. Ducheyne, P., and Q. Qiu, "Bioactive ceramics: The effect of surface reactivity on bone formation and bone cell function," *Journal of Applied Biomaterials*, Vol. 20, no. 23-24, pp. 2287–2303, 1999.
36. Abbasian, M., B. Massoumi, R. Mohammad-Rezaei, H. Samadian, and M. Jaymand, "Scaffolding polymeric biomaterials: Are naturally occurring biological macromolecules more appropriate for tissue engineering?," *International Journal of Biological Macromolecules*, Vol. 134, pp. 673–694, 2019.
37. Kokubo, T., and H. Takadama, "How useful is sbf in predicting in vivo bone bioactivity?," *Biomaterials*, Vol. 27, no. 15, pp. 2907–2915, 2006.
38. Araujo, J. V., A. Martins, I. B. Leonor, E. D. Pinho, R. L. Reis, and N. M. Neves, "Surface controlled biomimetic coating of polycaprolactone nanofiber meshes to be used as bone extracellular matrix analogues," *Journal of Biomaterials Science, Polymer Edition*, Vol. 19, no. 10, pp. 1261–1278, 2008.
39. Adepu, S., N. Dhiman, A. Laha, C. S. Sharma, S. Ramakrishna, and M. Khandelwal, "Three-dimensional bioprinting for bone tissue regeneration," *Current Opinion in Biomedical Engineering*, Vol. 2, pp. 22–28, Jul 2017.
40. Midha, S., M. Dalela, D. Sybil, P. Patra, and S. Mohanty, "Advances in three-dimensional bioprinting of bone: Progress and challenges," *Journal of Tissue Engineering and Regenerative Medicine*, Vol. 13, no. 6, pp. 925–945, 2019.
41. Mishra, S., and M. L. Knothe Tate, "Effect of lacunocanalicular architecture on hydraulic conductance in bone tissue: Implications for bone health and evolution," *Anatomical Record - Part A Discoveries in Molecular, Cellular, and Evolutionary Biology*, Vol. 273, no. 2, pp. 752–762, 2003.
42. Boyan, B. D., T. W. Hummert, D. D. Dean, and Z. Schwartz, "Role of material surfaces in regulating bone and cartilage cell response," *Biomaterials*, Vol. 17, no. 2, pp. 137–146, 1996.

43. Chehroudi, B., J. Ratkay, and D. Brunette, "The role of implant surface geometry on mineralization in vivo and in vitro - a transmission and scanning electron-microscopic study," *Cells and Materials*, Vol. 2, no. 2, pp. 89–104, 1992.
44. Ilan, D. I., and A. L. Ladd, "Bone graft substitutes," *Operative Techniques in Plastic and Reconstructive Surgery*, Vol. 9, no. 4, pp. 151–160, 2002.
45. Harrison, M. J. J., and K. L., "The effect of crystalline morphology on the degradation of polycaprolactone in a solution of phosphate buffer and lipase," *Polymers for Advanced Technologies*, pp. 229–236, Nov 2008.
46. Roohani-Esfahani, S. I., P. Newman, and H. Zreiqat, "Design and fabrication of 3d printed scaffolds with a mechanical strength comparable to cortical bone to repair large bone defects," *Scientific Reports*, Vol. 6, pp. 1–8, Jan 2016.
47. Tanahashi, M., T. Yao, T. Kokubo, M. Minoda, T. Miyamoto, T. Nakamura, and T. Yamamuro, "Apatite coated on organic polymers by biomimetic process: Improvement in its adhesion to substrate by naoh treatment," *Journal of Applied Biomaterials*, Vol. 5, no. 4, pp. 339–347, 1994.
48. Nagano, M., T. Kitsugi, T. Nakamura, T. Kokubo, and M. Tanahashi, "Bone bonding ability of an apatite-coated polymer produced using a biomimetic method: A mechanical and histological study in vivo," *Journal of Biomedical Materials Research*, Vol. 31, no. 4, pp. 487–494, 1996.
49. Reis, R. L., A. M. Cunha, M. H. Fernandes, and R. N. Correia, "Treatments to induce the nucleation and growth of apatite-like layers on polymeric surfaces and foams," *Journal of Materials Science: Materials in Medicine*, Vol. 8, no. 12, pp. 897–905, 1997.
50. Mondéjar, S. P., A. Kovtun, and M. Epple, "Lanthanide-doped calcium phosphate nanoparticles with high internal crystallinity and with a shell of dna as fluorescent probes in cell experiments," *Journal of Materials Chemistry*, Vol. 17, no. 39, pp. 4153–4159, 2007.
51. Oyane, A., M. Nakamura, I. Sakamaki, Y. Shimizu, S. Miyata, and H. Miyaji, "Laser-assisted wet coating of calcium phosphate for surface-functionalization of peek," *PLoS ONE*, Vol. 13, no. 10, pp. 1–15, 2018.
52. Zhao, F., W. L. Grayson, T. Ma, B. Bunnell, and W. W. Lu, "Effects of hydroxyapatite in 3-d chitosan-gelatin polymer network on human mesenchymal stem cell construct development," *Biomaterials*, Vol. 27, no. 9, pp. 1859–1867, 2006.
53. Aliah, N. N., and M. Ansari, "Thermal analysis on characterization of polycaprolactone (pcl) â chitosan scaffold for tissue engineering," *International Journal of Scientific Research Engineering & Technology*, Vol. 6, no. 2, pp. 76–80, 2007.
54. Balu, R., T. S. Sampath Kumar, M. Ramalingam, and S. Ramakrishna, "Electrospun polycaprolactone/poly(1,4-butylene adipate-co-polycaprolactam) blends: Potential biodegradable scaffold for bone tissue regeneration," *Journal of Biomaterials and Tissue Engineering*, Vol. 1, no. 1, pp. 30–39, 2011.
55. Ambrosio, A. M., J. S. Sahota, Y. Khan, and C. T. Laurencin, "Adsorption of a textile dye on synthesized calcium deficient hydroxyapatite: Kinetic and thermodynamic studies," *Journal of Materials and Environmental Science*, Vol. 7, no. 11, pp. 4049–4063, 2016.
56. Gunpath, U., and H. Le, "Composite coatings for implants and tissue engineering scaffolds," *Procedia CIRP*, Vol. 67, no. 1997, pp. 111–138, 2017.